



Durham E-Theses

Ageing Biomarkers and their role in the development of an aged skin model in vitro

HUNTER-FEATHERSTONE, EVE,FLOYD

How to cite:

HUNTER-FEATHERSTONE, EVE,FLOYD (2017) *Ageing Biomarkers and their role in the development of an aged skin model in vitro*, Durham theses, Durham University. Available at Durham E-Theses Online: <http://etheses.dur.ac.uk/12341/>

Use policy

The full-text may be used and/or reproduced, and given to third parties in any format or medium, without prior permission or charge, for personal research or study, educational, or not-for-profit purposes provided that:

- a full bibliographic reference is made to the original source
- a [link](#) is made to the metadata record in Durham E-Theses
- the full-text is not changed in any way

The full-text must not be sold in any format or medium without the formal permission of the copyright holders.

Please consult the [full Durham E-Theses policy](#) for further details.

Academic Support Office, Durham University, University Office, Old Elvet, Durham DH1 3HP
e-mail: e-theses.admin@dur.ac.uk Tel: +44 0191 334 6107
<http://etheses.dur.ac.uk>



Ageing Biomarkers and their role
in the development of an aged
skin model *in vitro*

Eve Hunter-Featherstone
Masters Thesis

Supervisor: Prof. Stefan Przyborski
Department of Biosciences, Durham
University
2017

Abstract

Ageing describes the decreased functionality and inability to resist physiological stress exhibited by all tissues as they get older. The skin is no exception to this rule; experiencing both intrinsic and extrinsic ageing which results in the remodelling of the entire tissue through degradation of extracellular matrix (ECM) proteins. In recent years, advancements in 2D cell culture and 3D bioengineered skin models have begun to help us better understand the workings of human skin. However, there is a need for the development of an 'aged' skin model, which would offer an innovative opportunity to further explore the ageing process, in a realistic, reproducible and readily available format. A key aspect of any ageing model, is that it must exhibit changes in biomarkers that have been linked to *in vivo* skin ageing. With this in mind, this project aims to identify key biomarkers of ageing through analysis of both mRNA and protein levels; specifically focusing on the dermal compartment.

Contents

Introduction	1
1.1 Skin ageing	3
1.1.1 Intrinsic ageing.....	3
1.1.2 Extrinsic ageing	4
1.2 Ageing biomarkers of the skin	7
1.2.1 Biomarkers of ECM degradation	7
1.2.2 Progerin as a potential ageing biomarker.....	8
1.3 Skin models.....	10
1.3.1 Current skin models	10
1.3.2 Alvetex® technology	11
1.3.3 Ageing skin models.....	11
1.4 Aims and objectives	13
Materials and Methods	14
2.1 2D cell culture	14
2.1.1 Human dermal fibroblasts, neonatal (HDFn)	14
2.1.2 Human mammary gland/breast tissue carcinoma line MDA-MB- 231....	14
2.1.3 Coriell Biorepository, human dermal fibroblasts	14
2.2 Irradiation of HDFn	16
2.3 3D cell culture	16
2.3.1 Alvetex® 3D dermal equivalents, HDFn.....	16
2.4 Immunocytochemistry	17
2.4.1 Immunocytochemistry.....	17
2.5 Histology	18
2.5.1 Paraffin embedding of Alvetex® 3D cultures.....	18
2.5.2 OCT embedding of Alvetex® 3D cultures.....	19
2.5.3 Haematoxylin and Eosin Staining.....	19

2.5.4	Immunohistochemistry of paraffin embedded human skin samples.....	19
2.5.5	Immunohistochemistry of frozen human skin samples	20
2.6	Western Blot.....	22
2.6.1	Preparation of lysates from flask cultures.....	22
2.6.2	Preparation of lysates from Alvetex® cultures.....	22
2.6.3	Sample and gel preparation	22
2.6.4	Electrophoresis and electrotransfer.....	23
2.7	RT-qPCR	25
2.7.1	Preparation of lysates from flask cultures.....	25
2.7.2	RNA extraction.....	25
2.7.3	Reverse transcription	26
2.7.4	qPCR.....	26
2.8	Transcriptomic data analysis	27
Results	29
3.1	Analysis of irradiation-induced senescent phenotype	29
3.2	Identifying ageing biomarkers.....	32
3.3	Expression of ageing biomarkers in human skin.....	33
3.4	Ageing biomarkers in irradiation-induced senescent HDFn	39
3.4.1	Changes in gene expression.....	39
3.4.2	Changes in protein levels	40
3.5	Ageing biomarkers in young and old HDF	42
3.5.1	Changes in gene expression.....	42
3.5.2	Changes in protein levels	43
3.6	Progerin expression in HDF	45
3.6.1	Nuclear circularity and abnormalities	45
3.6.2	Progerin protein levels	49
3.7	Ageing biomarkers in irradiation-induced senescent HDFn grown on a 3D Alvetex® scaffold	50

Discussion	52
4.1 HDFn irradiated and then cultured for 10 days still expressed Ki67	52
4.2 Changes in ageing biomarkers in irradiated HDFn differed from photoexposed TXP results	54
4.2.1 Gene expression changes of ageing biomarkers	54
4.2.2 Changes in protein level of ageing biomarkers.....	56
4.3 Changes in ageing biomarkers in young and old HDF differed from photoexposed TXP results	59
4.3.1 Gene expression changes of ageing biomarkers	59
4.3.2 Changes in protein level of ageing biomarkers.....	60
4.4 Nuclear abnormalities were observed in irradiated and old HDF, but progerin levels showed no change	62
4.4.1 Nuclear circularity was a poor indicator of nuclear abnormalities	62
4.4.2 The number of nuclear abnormalities did not correlate with progerin levels	63
4.5 HDFn cultured on Alvetex® scaffolds exhibited some differences in ageing biomarkers compared to 2D cultures.....	65
4.5.1 Irradiated 3D cultured HDFn still expressed lamin A	65
4.5.2 3D cultured HDFn produced a single band for collagen I in Western blot analysis	66
4.6 Analysis of human skin samples revealed the same changes in biomarkers as observed <i>in vitro</i>	67
 Conclusion and Further Directions	 69

List of Figures

1	Remodelling of the ECM in intrinsically and extrinsically aged skin.....	5
2	Change in cell proliferation after irradiation.....	30
3	Analysis of Ki67 expression in control and irradiated HDFn.....	31
4	H&E stains of human skin samples taken from the arm biopsies of young and old donors.....	34
5	Immunofluorescence analysis of collagen I expression in young and old human skin samples.....	35
6	Immunofluorescence analysis of collagen IV expression in young and old human skin samples.....	36
7	Immunofluorescence analysis of elastin expression in young and old human skin samples.....	37
8	Immunofluorescence analysis of lamin A/C expression in young and old human skin samples.....	38
9	qPCR analysis of biomarker expression in control and irradiated HDFn	39
10	Western blot analysis of biomarker expression in control and irradiated HDFn.....	41
11	qPCR analysis of biomarker expression in young and old HDF	42
12	Western blot analysis of biomarker expression in young and old HDF	44
13	Lamin A/C staining revealed abnormalities in the nuclear envelope.....	46
14	Nuclear circularity and visible abnormality analysis for control and irradiated HDFn.....	47
15	Nuclear circularity and visible abnormality analysis of young and old HDF .	48
16	Western blot analysis of progerin expression in HDF.....	49
17	Western blot analysis of ageing biomarker expression in control and irradiated HDFn grown on a 3D Alvetex® scaffold.....	50
18	Changes in Ki67 expression in irradiated HDFn	53

List of Tables

1	Non-foetal human dermal fibroblast lines obtained from the NIGMS Human Genetic Cell Repository	14
2	Settings used on X-ray machine to achieve required dosage (Gy).....	16
3	Primary and secondary antibodies used in immunocytochemistry	17
4	Primary and secondary antibodies used in immunohistochemistry on paraffin embedded wax sections	20
5	Primary and secondary antibodies used in immunohistochemistry on OCT embedded sections	21
6	Primary and secondary antibodies used in Western blot.....	24
7	TaqMan primers used in qPCR.....	27
8	Changes in ageing biomarker mRNA expression patterns in the dermis of young and old human skin samples.....	32

Abbreviations

x *g* – Relative Centrifugal Force

AP-1 – Activator Protein 1

BSA – Bovine Serum Albumin

Ct – Cycle Threshold

CYP26 – Cytochrome *P*450 26

DEJ – Dermal-Epidermal Junction

DMEM – Dulbecco's Modified Eagle Medium

ECM – Extracellular Matrix

EGF – Epidermal Growth Factor

FBS – Foetal Bovine Serum

GAGs – Glycosaminoglycans

GPa – Giga Pascal

HA – Hyaluronic Acid

HAS2 – Hyaluronic Acid Synthase 2

HDFn – Human Dermal Fibroblasts, neonatal

HGPS – Hutchinson-Gilford Progeria Syndrome

IL-1 α – Interleukin-1 α

kPa – Kilo Pascal

LSGS – Low Serum Growth Serum

M106 – Medium 106

MAPK – Mitogen-Activated Kinase Pathway

MEM – Minimal Essential Medium

MMP – Matrix Metalloproteinase

MPa – Mega Pascal

NEAAs – Non-Essential Amino Acids

OCT – Optimal Cutting Temperature compound

PBS – Phosphate-Buffered Saline

PFA – Paraformaldehyde

P&G – Proctor and Gamble

pVHL – Von Hippel-Lindau Protein

rpm – Revolutions per minute

RLTD – Relative Transcriptional Difference

ROS – Reactive Oxygen Species

RT – Reverse Transcription

(SA)- β -gal – Senescence-Associated β -Galactosidase

SASP – Senescence Associated Secretory Phenotype

SEM – Standard Error of the Mean

TIMP – Tissue Inhibitor of Metalloproteinases

TNF – Tumour Necrosis Factor

TXP – Transcriptomic

UVR – UV Radiation

VMSCs – Vascular Smooth Muscle Cells

WT - Wild Type

Yrs – Years Old

Acknowledgements

Firstly, my thanks go to my supervisor Professor Stefan Przyborski, who me gave the opportunity to pursue a project on an area that peaked my interest during my Undergraduate studies.

I am also extremely grateful to the rest of the laboratory members, who provided a strong support network that helped keep me moralised on the days when not everything went to plan. In particular, Dr Nicola Fullard, and Dr Mathilde Roger for helping me through to logistics of new experiments, and also to Lydia Costello, Nicole Darling, Matthew Freer, Rebecca Quelch, Antonio Romo-Morales, Kirsty Clarke, Lucy Smith, and Dr Fred Tholozan and Pam Ritchie.

I would also like to thank the members of the P&G collaboration from Cincinnati, Newcastle and Durham, for following my progress throughout the year, and providing invaluable advice.

Finally, I would like to thank my husband Ian Featherstone, for his patient love and support, and for listening to me practice countless presentations, despite not understanding them.

1. Introduction

The process of ageing is characterised as a decrease in functionality due to a failure to maintain homeostasis in response to physiological stress; causing the body to gradually decline. Research suggests that there is no one cause; genetics, exposure to environmental stresses and build-up of reactive oxygen species (ROS), all having been linked to resulting in the ageing phenotype (Mancini *et al.*, 2014). Like all tissues, skin can age intrinsically; resulting in thinning of the dermis, build-up of senescent keratinocytes, and break down of collagen and elastic fibres; however, it also has a separate ageing process known as extrinsic ageing. The phenotype of wrinkled skin derived from extrinsic ageing is thought to be caused by exposure to UVB; with the effects being superimposed onto those seen in intrinsic ageing to accelerate the ageing process (Naylor *et al.*, 2011).

Skin's primary function is to act as a barrier; both keeping pathogenic organisms out of the body, and preventing heat and water loss from within. As it ages, this barrier function is compromised; subject to the physiological changes skin undergoes during its lifetime (Proksch *et al.*, 2008). Skin is composed of two distinct layers; the avascular epidermis, made up of keratinocytes, and the vascular and relatively acellular dermis, made up of fibroblasts. These two layers are joined at the DEJ, where the epidermis is anchored to a collagen IV-rich basement membrane via hemidesmosomes, and the dermis is bound through fibrillin-rich microfibril bundles and collagen VII fibrils (Naylor *et al.*, 2011). The extracellular matrix (ECM) components of the dermis are thought to be secreted by dermal fibroblasts, and it is the changes in this ECM that characterises skin ageing (Brun *et al.*, 2015). Collagens I and III are the most abundant ECM proteins in the dermis, and co-polymerise to provide the tissue's tensile strength. In addition, skin elasticity (resilience and compliancy) is provided by the presence of an elastic fibre system; fibrillin-rich oxytalan fibres at the DEJ, perpendicularly merging with elastin in the reticular dermis to provide a complex architecture that enables the skin to deform and recoil. Finally, the group of carbohydrates, collectively referred to as GAGs help to maintain skin hydration (Naylor *et al.*, 2011). Unlike the majority of other tissues, skin undergoes both an intrinsic and extrinsic ageing process.

Ageing biomarkers are biological parameters that can be used to predict the rate of ageing within a tissue (Johnson, 2006). There are currently several established biomarkers of skin ageing, that vary depending on UV exposure. Intrinsic ageing of

the skin over time, results in the gradual degradation of collagens I, III and IV, and elastic fibres, and the loss of oligosaccharides, which impacts the skin's ability to retain water. In conjunction, these changes produce the aged phenotype of wrinkled, stiffened skin that is less able to recoil. Extrinsic ageing is triggered as a result of exposure to UV radiation, and results in a distinctly different remodeling event; including both catabolic and anabolic mechanisms (Takeuchi and R nger, 2013). These events are dose dependent; severe photoageing resulting in the additional loss of collagen VII at the dermal-epidermal junction (DEJ), and the increase and redistribution of glycosaminoglycans (GAGs) to co-localise with the elastic fibre system. This network is also remodeled; severe photoageing leading to the accumulation of disorganised elastic fibre proteins in the reticular dermis (Kohl *et al.*, 2011).

However, it is not just UVB which may have an impact on skin ageing. The effects of UVA are poorly understood and have been previously linked to the production of ROS. However, a study by Takeuchi and R nger (Takeuchi & R nger, 2013), revealed that exposing primary human fibroblasts (HF_p) to long-term doses of UVA led to an increased expression of progerin. Progerin is the truncated form of the protein lamin A produced by sufferers of Hutchinson Gilford Progeria Syndrome (HGPS); a disease in which the ageing process is accelerated. Studies such as that carried out by Scaffidi and Misteli (Scaffidi & Misteli, 2006), have shown that progerin may play a part in cell senescence and the normal ageing process of skin; raising the question as to whether progerin could be used as a biomarker for human skin ageing.

The development of 3D biosynthetic skin models, could enable us to gain a better understanding of the ageing process in skin. Currently, there are two main types of skin substitute; those grown from tissue samples, and those grown from cells. The former are primarily used for skin grafts in burns patients who only have small amounts of undamaged skin available (Jean *et al.*, 2011). However, this method relies on the availability of tissue biopsies, and is not realistic in terms of research due to poor cost-effectiveness and the limited availability of donors. Consequently, researchers have begun to experiment with developing full thickness skin models grown from fibroblasts and keratinocytes. This is termed the 'self-assembly' approach; fibroblasts are cultured on a scaffold for several days, then keratinocytes are seeded on top and the scaffold is raised to the air liquid interface (Dos Santos *et al.*, 2015). Traditionally, these scaffolds are formed using a collagen matrix (Brohem *et al.*, 2011). However, a new leading player in the production of 3D scaffolds is

Alvetex®; a polystyrene, highly porous membrane on which cells are able to interact with each other in a way that mimics cell behaviour *in vivo* (Knight *et al.*, 2011).

1.1 Skin ageing

1.1.1 Intrinsic ageing

Ageing is a progressive process that leads to loss of the physiological function and structural integrity of a tissue. Over time, the skin undergoes ageing as a result of internal factors that impact its organization and mechanical veracity; this is known as intrinsic ageing. Intrinsically aged skin is characterized by extracellular atrophy in both the epidermis and the dermis, loss of rete ridges, and a decrease in cell number; particularly fibroblasts and mast cells in the dermal compartment (Baumann, 2007). As previously mentioned, a large component of skin is the dermal ECM, which is comprised of collagen fibres, elastic fibres, and GAGs (Mancini *et al.*, 2014), and respectively provide skin with its structural integrity, elasticity, and hydration. During ageing, these ECM components are gradually degraded (**Figure 1**), which contributes to the appearance of aged skin; specifically wrinkling, drying, and increased fragility, as well as inferior wound healing (Jenkins, 2002). In intrinsic ageing, these changes are attributed to a decrease in the proliferation of skin cells, decreased dermal synthesis of ECM proteins, and an increase in the expression of collagen-degrading enzymes (Jenkins, 2002).

A key factor in the inducement of these changes, is cellular senescence; a natural phenomenon in which cells enter an irreversible state of cell cycle arrest following a set number of population doublings (von Zglinicki *et al.*, 2005), locking them in the G1 phase of the cell cycle. Key biomarkers of senescence, include repression of genes required for progression out of the G1 phase, and upregulation of negative growth regulators such as p21 and p16. In senescent fibroblasts, genes such as c-Fos proto-oncogene, ID1 and ID2, and E2F transcription factor components, are down-regulated, whilst in keratinocytes an age-related reduction in receptor phosphorylation and epidermal growth factor (EGF) binding is observed (Jenkins, 2002). Moreover, senescent cells are also known to secrete chemokines, cytokines, and growth factors; collectively known as senescence-associated secretory phenotype (SASP) factors. These SASP components, have been found to have a paracrine effect on local cells; ultimately inducing cellular senescence via a mechanism known as the bystander effect (Tasdemir & Lowe, 2013). As

senescence provides an immunity to apoptosis, intrinsic ageing is thus associated with a gradual accumulation of senescent cells (Jenkins, 2002). The main effect of having a high number of senescent cells in skin, is that it changes the balance of collagen turnover. In presenescent cells, expression of collagen-degrading MMPs is relatively low, whilst MMP inhibitors TIMPs are expressed at a relatively high level (Jenkins, 2002). However, in senescent cells this is reversed; resulting in an increase in collagen degradation due to MMP upregulation (Rodier & Campisi, 2011). The combination of a reduced cell number, and an increase in senescent cells, results in both a decrease in ECM production, and an increase in collagen breakdown; ultimately facilitating the process of intrinsic ageing (Mancini *et al.*, 2014).

Cellular senescence can arise as a result of the cell reaching its Hayflick limit; an inbuilt cut off point in its capacity to divide (Shay & Wright, 2000). Nonetheless, one of the most prevalent causes of premature senescence, is exposure to oxidative stress, and the subsequent DNA damage (Poljšak *et al.*, 2012). Oxidative stress occurs as a result of an imbalance between antioxidative activity, and production of ROS. Most ROS are produced as a byproduct of respiration in the mitochondria, and as cells age, these mitochondria become 'leaky'; enabling more ROS to escape (Poljšak *et al.*, 2012). Exposure to ROS has been linked to decreased proliferation, and premature senescence in dermal fibroblasts (Stöckl *et al.*, 2006). Consequently, combined with a natural decrease in the efficiency of DNA damage repair mechanisms, oxidative stress has been hallmarked as the most important contributor in chronological skin ageing (Poljšak *et al.*, 2012).

1.1.2 Extrinsic ageing

Extrinsically aged skin describes areas such as the face, chest, arms and hands, which are exposed to the sun, and thus subjected to prolonged dosage of UV radiation (UVR). Physically, these areas appear different to non-exposed, intrinsically aged skin which tends to be relatively unblemished and smooth, with slight lining (Baumann, 2007). However, extrinsically aged skin is characterised by obvious wrinkles, changes to the pigmentation, and loss of elasticity combined with increased fragility of the tissue (Baumann, 2007). At a structural level, photoageing results in both anabolic and catabolic remodelling of the ECM; with a significant loss of both dermal collagens, and collagen VII at the DEJ, combined with an increase in dermal GAG content, which co-localises with abundant and disorganised elastic fibres (**Figure 1**, Naylor *et al.*, 2011).

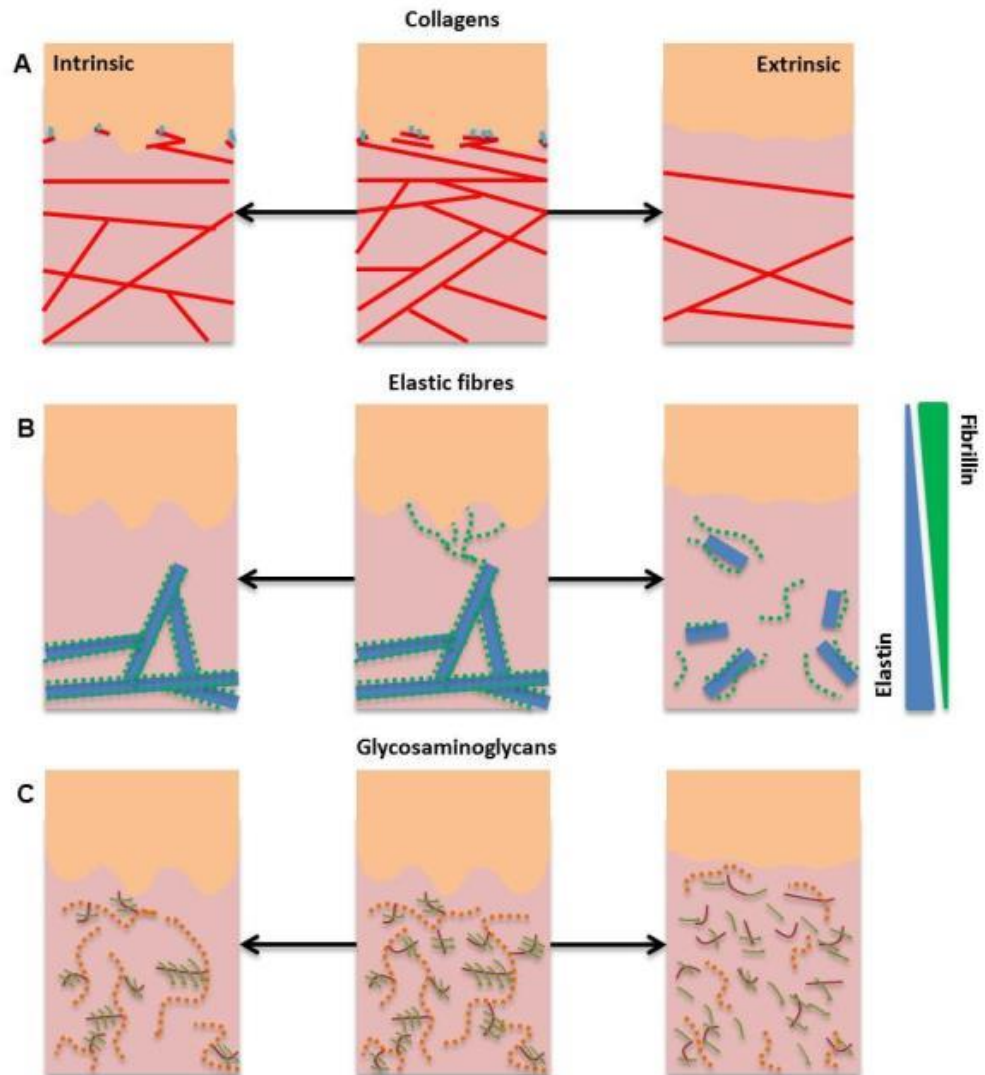


Figure 1: Remodelling of the ECM in intrinsically and extrinsically aged skin

ECM remodelling is a key feature of ageing in skin tissue. Intrinsic ageing is characterised by a decrease in collagen expression (A – collagen shown in red), decreased elastic fibres, particularly fibrillin (B – elastin shown in blue and fibrillin in green), and reduction of GAGs (C – hyaluronic acid shown in orange and chondroitin sulphate glycosaminoglycan side chains shown in brown and green). Extrinsic ageing exhibits both anabolic and catabolic changes, with a significant loss of dermal collagen, and anchoring fibrils at the DEJ (A). Elastic fibres are remodelled and redistributed in disorganised aggregates (B), whilst GAG levels are increased, and components are redistributed across the dermis to colocalise with elastic fibres (C). Figure adapted from Naylor *et al.* (2011).

The connection between oxidative stress and skin ageing has already been alluded to with regards to chronological ageing. However, oxidative stress also plays a significant role in extrinsic ageing as a consequence of UVR exposure. UVR triggers the production of ROS, and once their level exceeds the antioxidant capacity of the body, oxidative stress occurs. As UVR promotes the production of a greater number of ROS than would be produced intrinsically, onset of oxidative stress occurs much sooner than would be observed in photoprotected regions of skin. As a result, the DNA damage associated with oxidation begins to accumulate at an earlier age in photoexposed skin; explaining the differences in severity of the ageing process (Poljšak & Dahmane, 2012). When UVR comes into contact with cells, it is absorbed by DNA which subsequently leads to the inactivation of DNA functions due to the production of photoproducts such as thymine and pyrimidine dimers (Calleja-Agius, 2013). In keratinocytes, UVR increases superoxide production by upregulating the activity of xanthine oxidase (Halliday, 2005). Moreover, UVR also triggers a decrease in the activity of enzymatic antioxidants such as catalase; leading to an increase in ROS, but a diminished ability to degrade them (Poljšak & Dahmane, 2012).

In addition to increasing ROS production, UVR also leads to inflammation of the skin by augmenting blood flow; resulting in an influx of leukocytes. This is primarily promoted by lipid peroxidation, which leads to an increase in prostaglandin production (Tsourelis-Nikita *et al.*, 2006). In addition, UVR has also been linked to increased levels of interleukin-1 α (IL-1 α) and tumour necrosis factor (TNF); both of which promote an inflammatory response (Halliday, 2005). The recruited leukocytes secrete further ROS; increasing the levels of oxidative stress within the tissue (Reuter *et al.*, 2010). One effect of this, is the activation of growth factor receptors and cytokines, which activates the mitogen-activated kinase pathway (MAPK). The MAPK pathway induces activator protein 1 (AP-1) transcription, which subsequently upregulates the MMP genes (Tsourelis-Nikita *et al.*, 2006). Parallel to this process, ROS also act to deactivate TIMPs; thus increasing the amount of collagen degradation in photoexposed skin, compared to intrinsically aged tissue. In a final mechanism, loss of collagen in the dermis, effects the stimuli being received by fibroblasts; resulting in altered gene expression that results in less collagen being produced by the cells (Fisher *et al.*, 2009).

In terms of changes to elastin, intrinsic ageing is shown to result in a slow degradation of elastic fibres over time. However, in photoexposed skin, elastin levels are observed to increase and form disorganised aggregates (Naylor *et al.*,

2011). Studies have shown that, unlike the collagens, UVR exposure induces an increase in elastin expression in the skin (Seite *et al.*, 2006). In conjunction with this, it has also been found that areas of elastin that experience UV damage, are subsequently bound by lysozymes, which act to protect elastin from degradation (Seite *et al.*, 2006). Consequently, UVR induces both an upregulation of elastin production, whilst damaged elastin fibres are unable to be cleared; explaining the abnormal elastic fibre deposition observed in extrinsically aged skin. Finally, dermal GAG content has also been observed to increase in photoageing; however, the mechanism behind this is still poorly understood (Oh *et al.*, 2011).

1.2 Ageing biomarkers of the skin

In 1988, Baker and Sprott stated that, “A *Biomarker of Aging (BoA)* is a biological parameter of an organism that either alone or in some multivariate composite will, in the absence of disease, better predict functional capability at some late age, than will chronological age” (Baker and Sprott, 1988). However, in reality, this statement is very broad, and fails to take into account that each organ ages differently and thus will exhibit different biomarkers. In terms of skin, both intrinsic and extrinsic mechanisms take place during ageing, and therefore even in this one tissue, there are multiple different biomarkers depending on which area of the body is examined.

1.2.1 Biomarkers of ECM degradation

In the previous discussion on skin ageing (1.1), the majority of the key ageing biomarkers in both intrinsic and extrinsic ageing have already been introduced. Most significant, are those changes in ECM components such as the collagens, elastic fibres and GAGs; all three elements decreasing in intrinsic ageing, whilst in extrinsic, collagen degradation is accelerated, and elastin and GAG content increases (Mancini *et al.*, 2014). In addition, proteins such as MMPs and TIMPs, which play a key role in controlling collagen turnover are important biomarkers, with MMPs increasing with age, and TIMPs decreasing; this being exacerbated in photoexposed skin (Fisher *et al.*, 2014). Furthermore, it has also been mentioned that skin ageing is characterised by accumulation of senescent cells, and thus biomarkers of senescence such as p16^{INK4a}, p21 (Ressler, 2006) and senescence-associated β -galactosidase (SA- β -Gal) could also be biomarkers of tissue-wide ageing (Debacq-Chainiaux *et al.*, 2009). Finally, another significant component of ageing is oxidative stress, and thus inflammatory cytokines and enzymes involved

in antioxidation have been targeted as biomarkers of skin ageing; an example being TNF- α ; a marker of inflammation that has been observed to increase with age (Gonzalo-Calvo *et al.*, 2010).

1.2.2 Progerin as a potential ageing biomarker

The *LMNA* gene is located on chromosome 1, and encodes the A-type lamins; predominantly the major isoforms lamin A and lamin C. However, it is highly prone to mutation; as observed in sufferers of HGPS, where a de novo mutation in codon 608 of exon 11, changes nucleotide 1824 from a cysteine to a thymine. This introduces a cryptic splice site, which produces a truncated form of lamin A known as progerin (Meredith *et al.*, 2008). Lamin A is part of the nuclear envelope scaffold that maintains the integrity and structure of the nucleus, and is targeted to the nuclear membrane through the post-translation addition of a farnesyl group. This farnesyl group is then cleaved by an endoprotease, ZMPSTE24; enabling lamin A to migrate and interact with lamins B and C to form the scaffold. However, in the truncated progerin, the endoprotease cleavage site has been lost, meaning that progerin becomes trapped at the nuclear membrane and cannot join the scaffold (Cao *et al.*, 2011). In addition, it exerts a dominant negative effect on lamin A by interacting with it so it cannot move from the membrane.

In HGPS, the expression of progerin results in an accelerated ageing phenotype, due to early apoptosis of cells as a result of the abnormal nuclear structure. In light of this, it is logical to question whether progerin expression plays a part in normal human ageing. In 2006, Scaffidi and Misteli looked at human skin fibroblasts taken from young (3 - 11yrs) and old (81 – 98yrs) donors. Using reverse transcriptase polymerase chain reaction (RT-PCR) with primers for exons 9 and 12, the team were able to amplify a truncated product. DNA sequencing confirmed it to be $\Delta 50$ lamin A (progerin). To validate this, a splicing reporter was transfected into cells from young and old donors; revealing that there was sporadic use of the cryptic splice site in healthy cells. However, no difference in the amount of progerin mRNA was observed between the young and the old donors; suggesting that there is no positive correlation between increased age and use of the cryptic splice site (Scaffidi & Misteli, 2006).

One possible explanation for this could be the proposed connection between progerin and the von Hippel-Lindau protein (pVHL); a component of a ubiquitin-ligase E3 that degrades targeted cellular proteins. In renal cancers where the *VHL*

gene is mutated, progerin protein levels are elevated (Jung *et al.*, 2013). Immunoprecipitation of pVHL and progerin has confirmed direct binding between the two, and pVHL levels have been found to be inversely correlated with progerin half-life (Jung *et al.*, 2013). Whilst the link between pVHL and progerin in an ageing context is yet to be explored; if pVHL levels do change with age, the fact it regulates post-translation, could explain why Scaffidi and Misteli (Scaffidi & Misteli, 2006) found no difference in mRNA levels between donors.

In a similar study, McClintock *et al.* (2007) examined progerin levels in fibroblasts taken from skin biopsies. Samples included newborn foreskin, and skin from donors aged 22 to 97 years. As with the Scaffidi study, McClintock *et al.* found that when they carried out RT-PCR analysis, $\Delta 50$ cDNA was detected in all samples, but with no age-related difference observed. Nevertheless, the team then carried out a Western blot analysis to measure the levels of protein present in the cell. They found that there was no progerin detected in young samples, despite the evidence that mRNA was being produced. However, progerin was detected in samples from elderly donors, with the amount actually seeming to increase the older the donor. These results seem to consolidate the theory that pVHL may have a role in age-related progerin elevation. Moreover, whilst the current evidence is inconclusive, it does appear that levels of progerin protein increase correlatively with age.

As mentioned previously, skin can be extrinsically aged through exposure to UV radiation. To explore the effects sun-exposure has on age-related progerin expression, Takeuchi and R nger (Takeuchi & R nger, 2013) irradiated fibroblasts (young, aged *in vivo* and aged *in vitro*) with both short-wave UVB and long-wave UVA. Historically, UVB has been viewed as the main cause of photoageing. However, recent studies have shown that UVA is in fact a major factor; being more abundant, penetrating deeper into the dermis and having the ability to travel through glass (Battie *et al.*, 2014). Takeuchi and R nger (Takeuchi & R nger, 2013) observed this; both high dose acute exposure, and low dose chronic exposure to UVA resulting in increased progerin production. Results revealed that UVA exposure led to higher levels of progerin mRNA but not of lamin A; suggesting that the damage caused by UVA irradiation results in increased usage of the cryptic splice site. However, the induction of progerin following low dose exposure was only observed in the aged cells (*in vivo* and *in vitro*); suggesting that prolonged exposure to UVA is of greater detriment to older individuals and cells reaching senescence; perhaps due to a reduced ability to repair DNA damage. Whilst previous studies

have tried to link progerin to intrinsic skin ageing, Takeuchi and R nger (Takeuchi & R nger, 2013) provide compelling evidence that progerin is actually produced as a result of extrinsic ageing. Whilst this negates the concept that the HGPS phenotype is a direct example of inherent accelerated ageing, it does provide a possible role for progerin as a biomarker for photoageing in skin.

1.3 Skin models

Whilst our knowledge of the skin is expansive, it is by no means complete. For example, it is not fully understood how elastic fibres impact skin elasticity, and whilst it is accepted that dermal fibroblasts play a major role in ECM production, the changes undergone during ageing are still to be fully explored (Naylor *et al.*, 2011). In order to help target these gaps in our knowledge, scientists have begun to investigate the development of synthetic skin models *in vitro*. Not only would this allow an exploration into the mechanism behind skin ageing, it could also be used to look at various diseases such as psoriasis, eczema and melanoma and test possible drug treatments without the need for animal testing.

1.3.1 Current skin models

As mentioned previously, there are currently two main approaches to producing skin models; growing a skin substitute from tissue, or combining fibroblasts and keratinocytes on a scaffold (Jean *et al.*, 2011). The latter is rapidly gaining momentum as a technique for *in vitro* analysis of skin. Whilst 2D culture is a relatively easy method of investigating cells *in vitro*, it provides no information on the structure of a living tissue, and the behaviour of cells within it. In order to grow a skin model, fibroblasts are first cultured in 2D before being seeded onto a scaffold where they are cultured for around 7 days; enabling the cells to form a dermal compartment. Keratinocytes are then seeded on top of this dermis and the model is cultured at the air liquid interface to allow the epidermis to form (Dos Santos *et al.*, 2015). In some older skin models, fibroblasts were cultured without the use of a scaffold; being left to grow in the presence of ascorbic acid until they formed sheets of fibroblasts that layered on top of one another (Michel *et al.*, 1999). Whilst this technique is positive in that it does not involve the use of synthetic materials, it is not very physiologically accurate. The dermis is composed primarily of collagen and elastic fibres which ultimately provides skin tissue with its pliability and resilience (Naylor *et al.*, 2011). As a result, there are relatively few fibroblasts in comparison to

the amount of ECM. If skin models are grown without a scaffold, the resulting dermis will have an extremely high cell density in comparison to the *in vivo* tissue and as such this is perhaps not the most physiologically relevant simulation. Traditionally, the scaffolds used in skin models are created from a collagen matrix populated by fibroblasts (Brohem *et al.*, 2011). However, this too has its issues in that it prevents study into the ECM deposition of the fibroblasts under different conditions and thus hinders investigation into cell behaviour within the tissue. This has begun to lead to the development of scaffolds that are not formed from biological materials; enabling the tissue models to mature and deposit their own ECM.

1.3.2 Alvetex® technology

3D cell culture scaffolds are widely used in the production of skin models, as they enable cells to grow in a more physiological environment. As mentioned previously, some skin models are created to be utilised in a skin graft, and as such require a biodegradable scaffold (Jean *et al.*, 2007). However, for models that are to be used for routine cell culture and laboratory analysis, synthetic scaffolds offer a more controlled and robust environment that will not interfere with investigations into the tissue's ECM.

Alvetex® 3D scaffolds are formed of rigid polystyrene and are created by polymerisation in high internal phase emulsion (Knight *et al.*, 2011). The scaffold itself is only 200 µm thick, therefore ensuring that all cells within the scaffold receive an equal flow of nutrition, waste and gas exchange (Maltman & Przyborski, 2010). Moreover, the polystyrene is highly porous, with a void size of around 40 µm. These voids allow cells to interact with each other in a way that enables them to produce tissue-like structures within the scaffold (Knight & Przyborski, 2014). This *in vivo*-like interaction between cells provides the optimal environment to induce realistic gene expression. Consequently, using Alvetex® 3D scaffolds to explore ageing biomarkers, presents a favourable opportunity to develop a robust model of skin ageing.

1.3.3 Ageing skin models

One significant bonus of the self-assembly model, is that it can be manipulated to mimic aged skin and different pathogenic phenotypes. Dos Santos *et al.* (Dos Santos *et al.*, 2015) created an aged skin model through prolonged culture. Using fibroblasts and keratinocytes from young donors (1 - 2 years), samples were taken

at 42, 60, 75 and 120 days. They then measured thickness of the epidermis, and expression of proliferation marker Ki67, and epidermal differentiation markers p16INK4A, involucrin, filaggrin, loricrin and transglutaminase. Results showed that at day 120, the epidermis was significantly thinner than at day 42, and the number of Ki67 expressing cells had decreased. Moreover, comparison of keratinocyte proliferation marker expression with that of skin from young and old donors clearly suggested that day 120 samples exhibits an aged phenotype (Dos Santos *et al.*, 2015).

This ability to produce a model of aged skin provides scientists with the opportunity to begin exploring possible treatments and drugs to slow or reverse the ageing process. In terms of cosmetics, this is highly significant. In a recent study, Kim *et al.* (Kim *et al.*, 2015) grew young and senescent fibroblasts under 3D culture conditions. They observed that senescent fibroblasts had a lower migration rate and basal contractility than young cells. However, treatment of the aged cells with recombinant human epidermal growth factor (rhEGF) led to an increase in both their rate of migration and contractility, to a level similar and sometimes even higher than that of the young cells (Kim *et al.*, 2015).

Another promising study was carried out by Heise *et al.* (Heise *et al.*, 2006). There is strong evidence that all-*trans* retinoic acids (RA) have a reparative effect on UV-damaged skin when applied topically (Watson *et al.*, 2001). In the skin, all-*trans* Ras are metabolised into 4-oxo-RA, which has been shown to have pharmacological properties with regards to skin cells (Baron *et al.*, 2005). A key enzyme involved in the formation of this metabolite is cytochrome P450 26 (CYP26), and Heise *et al.* (Heise *et al.*, 2006) aimed their study at investigating its expression in human keratinocytes and dermal fibroblasts; comparing this directly to human skin samples, and 3D skin models. Fascinatingly, they observed that monolayer keratinocytes and fibroblasts expressed only minimal levels of CYP26, whilst 3D skin models were perceived to express significantly greater levels of the protein. Moreover, expression was localised to the basement membrane of the epidermis, which is where it is observed in human skin (Heise *et al.*, 2006). Consequently, this shows that basic 2D culture greatly limits our ability to study tissue behaviour *in vitro*. It is therefore clear that the future of cell culture lies in the development of 3D tissue equivalents, which replicate the *in vivo* environment.

1.4 Aims and objectives

The aim of this thesis is to identify key skin ageing biomarkers, and compare their changes in expression both *in vivo*, and *in vitro*, in both 2D and 3D culture. The main objectives of the project are:

1. To identify potential ageing biomarkers using microarray data provided by Proctor and Gamble (P&G).
2. To identify whether those biomarkers show similar changes in young and old human skin samples.
3. To compare ageing biomarkers in human skin, with expression in control and irradiated neonatal human dermal fibroblasts, and young and old adult human dermal fibroblasts
4. To compare progerin levels in control and irradiated neonatal human dermal fibroblasts, and young and old adult human dermal fibroblasts.
5. To compare the results from 2D culture, with biomarker changes in control and irradiated neonatal human dermal fibroblasts grown in 3D on Alvetex® scaffolds.

2. Materials and Methods

2.1 2D cell culture

2.1.1 Human dermal fibroblasts, neonatal (HDFn)

The HDFn (ThermoFisher Scientific, Cramlington, UK) were cultured in Medium 106 (M106, ThermoFisher) supplemented with 10ml Low Serum Growth Serum (LSGS, ThermoFisher) and 1ml Gentamicin/Amphotericin (ThermoFisher), following the supplier's instructions. Upon revival, 0.5×10^6 cells were seeded into a T175 flask (Greiner BioOne, Stonehouse, UK) containing 25ml pre-warmed medium. Flasks were incubated in a humidified atmosphere with 5% CO₂ at 37°C, medium changed every 2 to 3 days and passaged at 100% confluency. Cells were frozen down in 1ml cryovials (Starlab) at approximately 2×10^6 cells per ml in 1ml Synth-a-freeze (ThermoFisher) and kept at -150°C for long-term storage.

2.1.2 Human mammary gland/breast tissue carcinoma line MDA-MB-231

The human mammary gland/breast tissue carcinoma line MDA-MB-231 were grown in Dulbecco's Modified Eagle Medium (DMEM, Gibco™, ThermoFisher) supplemented with 10% Foetal Bovine Serum (FBS, Gibco™), 2mM L-glutamine (Lonza, Castleford, UK) and 1ml Penicillin/Streptomycin (Lonza). Upon revival, 0.75×10^6 to 2.25×10^6 cells were seeded into a T75 flask (Greiner BioOne) containing 12ml pre-warmed medium. Flasks were incubated in a humidified atmosphere with 5% CO₂ at 37°C, medium changed every 2 to 3 days and passaged at around 70 to 80% confluency. Cells were frozen down in 1ml cryovials (Starlab) at approximately 2×10^6 cells per ml in 1ml 90% FBS and 10% DMSO (Sigma-Aldrich) and kept at -150°C for long-term storage.

2.1.3 Coriell Biorepository, human dermal fibroblasts

Non-foetal human dermal fibroblasts were obtained from the NIGMS Human Genetic Cell Repository (Coriell Institute, Camden, USA). Six cell lines were utilized (see **Table 1**), all obtained from Caucasian male donors.

Cell line	Harvest site	Age (years)	Passage split ratio
GM03348	Inguinal area	10	1:6
GM00323	Arm	11	1:3
GM00316	Arm	12	1:3
AG06292	Arm	82	1:2
AG11651	Arm	82	1:3
AG12443	Arm	82	1:3

Table 1: Non-foetal human dermal fibroblasts lines obtained from the NIGMS Human Genetic Cell Repository (Coriell Institute, Camden, USA).

As per the supplier's instructions, GM03348 were grown in Minimal Essential Medium (MEM, Gibco™) containing Earle's Salts and Non-Essential Amino Acids (NEAAs) and supplemented with 10% FBS (Gibco™) and 1ml Penicillin/Streptomycin (Lonza). GM00323 and GM00316 were grown in MEM containing Earle's Salts and NEAAs and supplemented with 15% FBS (Gibco™) and 1ml Penicillin/Streptomycin (Lonza). AG06292, AG11651 and AG12443 were grown in MEM containing Hank's BSS and L-glutamine (Gibco™) and supplemented with 15% FBS (Gibco™), 26mM HEPES and 1ml Penicillin/Streptomycin (Lonza). Upon revival, the entire contents of the cryovials were seeded into T25 flasks (Greiner BioOne) containing 7ml pre-warmed medium. Flasks were incubated in a humidified atmosphere with 5% CO₂ at 37°C, medium changed every 2 to 3 days, and cells were passaged upon reaching 100% confluency. Cells were frozen down in 1ml cryovials (Starlab) at approximately 2x10⁶ cells per ml in 1ml of their usual medium, containing 10% DMSO (Sigma-Aldrich), and kept at -150°C for long-term storage.

2.2 Irradiation of HDFn

Prior to irradiation, HDFn were seeded into T75 flasks (0.2×10^6 per flask) and allowed to grow to approximately 70% confluency.

All irradiation was carried out using a Gulmay CP320 X-ray generator. Flasks were removed from the incubator and carried to the irradiator in an insulated box to keep them at an ambient temperature. The flasks were irradiated one at a time, and placed at a distance of 18 cm from the beam. The machine was set at 320kV, 10mA and the time was adjusted according to the dose required.

Time display	Actual time	Dose (Gy)
3.3	3m 18s	20.44
4.1	4m 6s	25.39
4.9	4m 54s	30.35
5.7	5m 42s	35.30

Table 2: Settings used on X-ray machine to achieve required dosage (Gy).

Following irradiation, the flasks were immediately returned to cell culture and rescued with pre-warmed M106 medium to reduce exposure to free radicals. The cells were medium changed three times a week as usual, and a stable senescent phenotype was observed from 10 days post-irradiation.

2.3 3D cell culture

2.3.1 Alvetex[®] 3D dermal equivalents, HDFn

Alvetex[®] in a 12-well insert (Reinnervate, Sedgefield, UK) were pre-treated by soaking in 70% ethanol for 2 to 5 minutes in a large petri dish. They were then washed with PBS, before being submerged in M106 medium until required. Standard dermal equivalents were made using passage 4 HDFn. The inserts were

transferred to a 6-well plate (Greiner Bio-one) and 100µl cell suspension, containing 0.5×10^5 cells, was seeded in a drop-wise manner onto each scaffold. The plate was incubated in a humidified atmosphere with 5% CO₂ at 37°C for 60 minutes. M106 medium was supplemented with 1% ascorbic acid and 5ng/ml TGFβ₁, and 10ml of this medium was added to each well; ensuring not to pipette it directly onto the scaffold. The plate was again incubated in a humidified atmosphere with 5% CO₂ at 37°C and grown for 28 days, with a full medium change every 3 to 4 days.

2.4 Immunocytochemistry

2.4.1 Immunocytochemistry

13 mm coverslips were placed into a 24-well plate and cells were seeded onto them at low density and grown for two days in 1ml of their relevant medium, incubated in a humidified atmosphere with 5% CO₂ at 37°C. Cells were fixed in 4% PFA for 15 minutes at room temperature. The coverslips were then washed three times in PBS for 5 minutes each. Blocking solution was made up of 20% neonatal calf serum (NCS) in PBS with 0.4% triton X-100 (Sigma) to allow permeabilization. Blocking was carried out for one hour at room temperature. Coverslips were incubated with the primary antibodies at 4°C overnight, in a humid atmosphere. Coverslips were washed in PBS three times for 10 minutes each. Coverslips were incubated for 60 minutes at room temperature with the secondary antibodies, then washed three times in PBS for 5 minutes each. They were then mounted onto slides using a drop of hard-set VECTASHIELD® anti-fade mounting medium with DAPI (VectorLaboratories). Slides were left to dry in a slide book at room temperature for 15 – 20 minutes then kept at 4°C until ready to image. All slides were imaged within 1 week of staining using an epifluorescent Zeiss Axioskop 40 microscope.

Antibody	Code	Manufacturer	Species and Isotype	Dilution
Anti-Lamin A/C	IQ332	ImmuQuest	Mouse monoclonal, IgG1	1:100
Anti-Ki67 (Alexa Fluor® 488)	ab154201	Abcam	Rabbit monoclonal, IgG	1:100
Anti-Mouse (Alexa Fluor® 488)	A21202	ThermoFisher	Donkey polyclonal, IgG (H + L)	1:1000

Table 3: Primary and secondary antibodies used in immunocytochemistry. All antibodies were diluted in blocking solution.

2.5 Histology

2.5.1 Paraffin embedding of Alvetex® 3D cultures

Alvetex® scaffold membranes were unclipped from their inserts and transferred to a 6-well plate using forceps. They were washed in PBS for approximately 2 minutes, then fixed in 4% PFA (Sigma-Aldrich) at 4°C overnight. Scaffolds were washed in PBS three times for 5 minutes, then dehydrated in 30%, 50%, 70%, 80%, 90% and 95% ethanol for 10 minutes each. The scaffolds were then transferred to cassettes and placed in a beaker of 100% ethanol for 30 minutes. The ethanol was replaced with HistoClear (ThermoFisher) before being left for a further 30 minutes. Half of the HistoClear (ThermoFisher) was emptied and replaced with molten paraffin wax (ThermoFisher) and the beaker was incubated in a 60°C oven for 30 minutes. Finally, the HistoClear:wax mixture was removed and replaced with 100% molten wax, and the beaker was incubated for a further 60 minutes in the 60°C oven.

The membranes were removed from the cassettes and laid flat on tin foil to allow them to dry. Once hardened, a scalpel blade was used to cut each membrane in half. Molten wax was poured into a dispmould and the membranes were orientated, using forceps, so that the cut edge of the membrane was in contact with the wax. The cassette was then placed over the membranes and molten wax was poured over the top until the mould was full. These were left to set at room

temperature overnight. All wax blocks were sectioned at 7µm using a Leica RM2125RT microtome and mounted onto Superfrost plus microscope slides (ThermoFisher, 4951PLUS4).

2.5.2 OCT embedding of Alvetex[®] 3D cultures

Alvetex[®] scaffold membranes were unclipped from their inserts and transferred to a 6-well plate using forceps then washed in PBS for approximately 5 minutes. A dispmould was filled with Optimal Cutting Temperature compound (OCT) and the membranes were cut in half using a scalpel. They were then inserted into the OCT using forceps, and orientated, so that the cut edge of the membrane was towards the bottom of the mould. The mould was then placed on a metal plate in a box containing liquid nitrogen. The block was left to set for 30 minutes then wrapped in tin foil and placed in a -80°C freezer until required. They were sectioned at 7µm using a cryostat, and mounted onto Superfrost plus microscope slides (ThermoFisher). After cutting, sections were left to dry at room temperature for 30 minutes then placed in the -20°C freezer until needed.

2.5.2 Haematoxylin and Eosin staining

Slides were deparaffanised in HistoClear (ThermoFisher) for 5 minutes, then gradually rehydrated; first being submerged in 100% ethanol for 2 minutes, then moved to 95% ethanol, 70% ethanol and deionised water for 1 minute each. The slides were soaked in Mayer's Haematoxylin for 5 minutes, then submerged in alkaline ethanol for 30 seconds. Samples were once again dehydrated through submersion in 70% ethanol and 95% ethanol for 30 seconds each. They were then soaked in eosin for 30 seconds and further dehydrated through submersion in 95% ethanol for two rounds of 10 seconds, 100% ethanol for 15 seconds, 100% ethanol for 30 seconds, then HistoClear (ThermoFisher) for two rounds of 30 seconds. Slides were mounted in DPX (VWR, Leicestershire, UK) using a glass coverslip and left to dry overnight at room temperature. Brightfield images were taken using a Leica ICC50HD microscope.

2.5.3 Immunohistochemistry of paraffin embedded human skin samples

Slides were submerged in HistoClear (ThermoFisher) for 10 minutes to deparaffinise them. Samples were then rehydrated for 5 minutes in 100% ethanol, 5 minutes in 70% ethanol and 5 minutes in PBS. Antigen retrieval was carried out through submersion in citrate buffer for 20 minutes at 95°C. Slides were gradually cooled

then transferred to a humidified box and blocked for 60 minutes at room temperature. Blocking solution was made up of 20% neonatal calf serum (NCS) in PBS with 0.4% triton X-100 (Sigma-Aldrich) to allow permeabilisation. Slides were incubated with the primary antibodies at 4°C overnight.

Slides were washed in PBS three times for 10 minutes each. Slides were incubated for 60 minutes at room temperature with the secondary antibodies, before being washed 3 times in PBS for 5 minutes each. Slides were mounted using hard-set VECTASHIELD® anti-fade mounting medium with DAPI (VectorLaboratories, Peterborough, UK) and a glass coverslip. Slides were left to dry in a slide book at room temperature for 15 – 20 minutes then kept at 4°C until ready to image. All slides were imaged within 1 week of staining using an epifluorescent Zeiss Axioskop 40 microscope.

Antibody	Code	Manufacturer	Species and Isotype	Dilution
Anti-Elastin	ab77804	Abcam	Mouse monoclonal, IgG1	1:100

Anti-Mouse (Alexa Fluor® 488)	A21202	ThermoFisher	Donkey polyclonal, IgG (H + L)	1:1000
-------------------------------	--------	--------------	--------------------------------	--------

Table 4: Primary and secondary antibodies used in immunohistochemistry on paraffin wax embedded sections. All antibodies were diluted in blocking solution.

2.5.4 Immunohistochemistry of frozen human skin samples

Frozen human skin samples were provided by Proctor and Gamble (P&G, Cincinnati, USA) and sectioned using a cryostat. Slides were stored at -80°C and allowed to thaw at room temperature for 30 minutes before use. They were then washed for 10 minutes in PBS, before being fixed. 4% PFA fixation was carried at room temperature for 10 minutes. For acetone fixation, ice-cold acetone was used and fixation took place at -20°C for 10 minutes. Slides were then washed three times in PBS for 5 minutes each.

Slides were transferred to a humidified box and blocked for 60 minutes at room

temperature. Blocking solution was made up of 20% neonatal calf serum (NCS) in PBS with 0.4% triton X-100 (Sigma-Aldrich) to allow permeabilisation. Slides were incubated with the primary antibodies at 4°C overnight. Slides were washed in TBST three times for 10 minutes each before being incubated for 60 minutes at room temperature with the secondary antibodies. Slides were washed 3 times in TBST for 5 minutes each, then mounted using hard-set VECTASHIELD® anti-fade mounting medium with DAPI (VectorLaboratories) and a glass coverslip. Slides were left to dry in a slide book at room temperature for 15 – 20 minutes then kept at 4°C until ready to image. All slides were imaged within 1 week of staining using an epifluorescent Zeiss Axioskop 40 microscope.

Antibody	Code	Manufacturer	Species and Isotype	Dilution	Fixation
Anti-Lamin A/C	IQ332	ImmuQuest	Mouse monoclonal, IgG1	1:100	PFA
Anti-Collagen IV	ab6586	Abcam	Rabbit polyclonal, IgG	1:100	Acetone
Anti-Collagen I	ab34710	Abcam	Rabbit polyclonal, IgG	1:100	PFA

Anti-Mouse (Alexa Fluor® 488)	A21202	ThermoFisher	Donkey polyclonal, IgG (H + L)	1:1000
Anti-Rabbit (Alexa Fluor® 488)	A21206	ThermoFisher	Donkey polyclonal, IgG (H + L)	1:1000

Table 5: Primary and secondary antibodies used in immunohistochemistry on OCT embedded sections. All antibodies were diluted in blocking solution.

2.6 Western Blot

2.6.1 Preparation of lysates from flask cultures

Protein lysates were made using 500µl RIPA buffer containing 5µl protease inhibitors.

RIPA buffer:

50 mM Tris

pH 7.5 – 8

150 mM NaCl

0.1% SDS

1% Nonidet P-40

0.5% Sodium-deoxycholate

1% Protease Inhibitors

All lysates were taken from a T75 flask. Flasks were rinsed with PBS then 500 µl of RIPA buffer was pipetted onto the base of the flask, and a cell scraper was used to dislodge cells. The resulting lysate was sonicated for 30 minutes, then spun in a 4°C centrifuge for 20 minutes at 13,000 rpm. The supernatant was removed and placed in a clean Eppendorf, before being stored in the -20°C freezer until required.

2.6.2 Preparation of lysates from Alvetex[®] cultures

Protein lysates were made using 500 µl RIPA buffer containing 5 µl protease inhibitors.

All lysates were taken from one whole Alvetex[®] scaffold. The scaffold disk was unclipped from the insert using forceps, and the membrane was rinsed in PBS before being transferred to an eppendorf containing 500 µl of buffer. Blunt forceps were used to break it up the scaffold, then the lysate was sonicated for 30 minutes, and spun in a 4°C centrifuge for 20 minutes at 13,000 rpm. The supernatant was removed (leaving the membrane behind) and the lysate was placed in a clean eppendorf, before being stored in the -20°C freezer until required.

2.6.3 Sample and gel preparation

A Bradford Assay was used to assess the protein concentration of each lysate, using protein standards of 1 mg, 0.75 mg, 0.5 mg, 0.25 mg and 0.125 mg (Biorad, Hemel Hempstead, UK), detergent compatible reagent, and RIPA buffer as a blank.

As per the manufacturer's instructions, samples were left to incubate with the reagent at room temperature for 10 minutes. A plate reader was then used to calculate the absorbency of each sample. Absorbance was read at 595 nm. 150 μ l of each sample was then diluted in 45 μ l of Laemmli and 5 μ l β -mercaptoethanol. The samples were then heated on a hot plate at 95°C for 10 minutes.

Gels were made using the following recipes – each recipe makes two 1.5 mm gels:

5% stacking gel:

dH₂O – 5.625 ml
Prosieve acrylimide – 750 μ l
1.5 M Tris pH 6.8 – 1 ml
10% SDS – 75 μ l
10% APS – 75 μ l
Temed – 7.5 μ l

8% resolving gel:

dH₂O – 11.4 ml
Prosieve acrylimide – 3.2 ml
1.5 M Tris pH 8.8 – 5 ml
10% SDS – 200 μ l
10% APS – 200 μ l
Temed – 10 μ l

10% resolving gel:

dH₂O – 10.6 ml
Prosieve acrylamide – 4 ml
1.5 M Tris pH 6.8 – 5 ml
10% SDS – 200 μ l
10% APS – 200 μ l
Temed – 10 μ l

2.6.4 Electrophoresis and electrotransfer

Gels were loaded with 20 μ g of protein, and run at 120 V. Transfer was carried out at 250 mA for approximately 90 minutes (for larger proteins, transfer was carried out at 4°C overnight using 15 V; increasing this to 30 V for 2 hours the next day).

Membranes were blocked for 60 minutes in 5% milk (semi-skimmed milk powder in TBST) and incubated with primary antibodies overnight in a 4°C cold room. The membrane was then washed three times for 10 minutes each in TBST before being incubated with the secondary antibody at room temperature for 60 minutes. The membrane was again washed three times for 10 minutes each in TBST.

The membrane was treated using either the Biorad ECL kit (Biorad) or the Amershan ECL kit (GE Healthcare, Chalfont ST Giles, UK), depending on the antigen being investigated.

Antibody	Code	Manufacturer	Species and Isotype	Dilution	Gel	Transfer
Anti-Lamin A/C	IQ332	ImmuQuest	Mouse monoclonal, IgG1	1:200	10%	105 mins
Anti-Progerin	ab153757	Abcam	Rabbit polyclonal, IgG	1:250	10%	105 mins
Anti-Collagen I	1310-01	SouthernBiotech	Goat, IgG	1:1000	8%	Overnight
Anti-Elastin	ab77804	Abcam	Mouse monoclonal, IgG1	1:1000	10%	105 mins
Anti-p21	ab7960	Abcam	Rabbit polyclonal, IgG	1:250	14%	90 mins
Anti-p16 ^{INK4a}	ab108349	Abcam	Rabbit monoclonal, IgG	1:2000	14%	90 mins
Anti-B actin	ab8224	Abcam	Mouse monoclonal, IgG	1:10,000	-	-

Anti-Mouse HRP	A4416	Sigma-Aldrich	Goat polyclonal, IgG (H + L)	1:3000
Anti-Rabbit HRP	711035152	Stratech	Donkey polyclonal, IgG (H + L)	1:3000

Table 6: Primary and secondary antibodies used in Western blot. All antibodies were diluted in 5% milk.

2.7 RT-qPCR

2.7.1 Preparation of lysates from flask cultures

RNA extraction was carried out using the ReliaPrep™ RNA Cell Miniprep System (Promega, Southampton, UK). RNA lysates were made using 500 µl BL buffer containing 5 µl 1-Thioglycerol.

All lysates were taken from a T75 flask. Flasks were rinsed with ice cold PBS then 500 µl of BL buffer was pipetted onto the base of the flask, and a cell scraper was used to dislodge cells. The resulting lysate was stored in a -80°C freezer until required.

2.7.2 RNA extraction

As mentioned previously, the ReliaPrep™ RNA Cell Miniprep System (Promega) was used to extract RNA, following the protocol provided with the kit. 170 µl of isopropanol was added to each lysate before they were transferred into a Minicolumn, which was placed inside a Collection Tube and centrifuged for 30 seconds at 14,000 x g. Liquid was discarded from the Collection Tube, and 500 µl RNA Wash Solution was added to each Minicolumn and they were centrifuged for another 30 seconds. The Collection Tubes were emptied and the DNase I incubation mix was prepared fresh by combining 24 µl Yellow Core Buffer, 3 µl 0.09 M MnCl₂ and 3 µl DNase I enzyme per sample. 30 µl of this mix was added directly to the membrane inside the Minicolumn and left to incubate for 15 minutes at room temperature. 200 µl Column Wash Solution was then added to each Minicolumn and they were spun at 14,000 x g for 15 seconds. 500 µl RNA Wash Solution and

the Minicolumns were centrifuged again for 30 seconds. The Collection Tubes were discarded and the Minicolumn were transferred to a new Collection Tube. 300 µl of RNA Wash Solution was added and the Minicolumns were centrifuged at high speed for 2 minutes. The Minicolumns were transferred to an Elution Tube and Nuclease-Free Water was added to the membrane; the volume of which was determined based on the approximate cell input range. The tubes were then centrifuged for a final time for 1 minute. The resulting RNA contained within the Elution Tube was then assessed for yield and quality using a Nanodrop. Samples with an A_{260}/A_{280} ratio of 1.7 – 2.1, and an A_{260}/A_{230} ratio of 1.8 – 2.2 were accepted and stored at -80°C until required.

2.7.3 Reverse transcription

Reverse Transcription (RT) was carried out using a High Capacity cDNA Reverse Transcription Kit (Applied Biosystems, ThermoFisher). The 2x RT master mix was prepared as instructed in the kit's protocol; 10 µl for each RNA sample. 10 µl of each sample was then added and the tubes were briefly centrifuged to ensure all liquid was at the bottom. The tubes were then placed in a 96-tube Eppendorf Mastercycler and run through the appropriate cycle: 10 minutes at 25°C, 120 minutes at 37°C, 5 minutes at 85°C and then held at 4°C. The resulting cDNA samples were stored in a -20°C freezer until required.

2.7.4 qPCR

cDNA samples were diluted 1:5 to produce a concentration of 10 ng/µl, i.e. 80 µl RNase-free water was added to each 20 µl sample. The TaqMan Master Mix (ThermoFisher) was then prepared:

Housekeeping Master Mix (n = 1) - for 15ng cDNA

AB TaqMan Universal Master Mix 2 with UNG (#444031) – 10 µl
TaqMan Primer – 1 µl
RNase-free H₂O - 7.5 µl

Master Mix (n = 1) - for 60ng cDNA

AB TaqMan Universal Master Mix 2 with UNG (#444031) – 10 µl
TaqMan Primer – 1 µl
RNase-free H₂O – 3 µl

18S was used as the housekeeping gene. 18.5 µl of the relevant Master Mix was added to each well of a 96-well PCR plate (Starlab), then 1.5 µl cDNA was added. For the genes under analysis, 14 µl of Master Mix was added to each well, and 6 µl of cDNA. RNase-free water was used as a blank. The plates were centrifuged at 1000 rpm for 3 minutes then the plate was placed in a PCR machine and a cycle was run.

Gene	Code
18S	HS03003631_g1
COL1A1	HS00164004_m1
COL4A1	HS00266237_m1
FBN1	HS00171191_m1
ELN	HS00355783_m1
MMP1	HS00899658_m1
TIMP1	HS00171558_m1
HAS2	HS00193435_m1

Table 7: TaqMan (ThermoFisher) primers used in qPCR.

Each cDNA sample was added to 3 wells, and the average ct value was calculated. This was then normalised to the housekeeping gene 18S, by subtracting the average housekeeping gene ct from the average ct of the gene being analysed, giving the Δ ct. The average Δ ct of each experimental group (i.e. irradiated HDFn) was normalised to the WT control group (i.e. untreated HDFn) using the equation $1/\text{POWER}(2, \text{ave}\Delta\text{ct}^x - \text{ave}\Delta\text{ct}^y)$.

2.8 Transcriptomic data analysis

P&G provided raw probe data from GeneChips used in the P&G Multi-decade and Ethnicity Study, and a Photoageing Ageing Pilot Study. Both studies were independent of one another and were conducted 9 years apart. Samples were taken from the arm and buttock regions of women aged 20, 30, 40, 50, 60 and

70yrs. Samples were analysed on Affymetrix HG-U219 GeneChips, with the results from the Photoageing Study including data from HG-U133Plus2 GeneChips, which were also used. Separate data was provided for full thickness, epidermal and dermal compartments. For the purpose of this study, analysis was focused on expression changes in the dermis (taken from the P&G MDE Study), and a comparison was made between photoprotected and photoexposed sites. Biomarkers were selected based on both their prevalence in the literature, and whether they had a significant P and/or Q value (< 0.05).

3. Results

3.1 Analysis of irradiation-induced senescent phenotype

HDFn exposed to a dose of 20.44 Gy were cultured in flasks for 10 days following irradiation, alongside untreated cells which were used as the control. Irradiation has been shown to cause irreversible cell cycle arrest which is ultimately the definition of cellular senescence. In order to assess the proliferative capacity of the irradiated HDFn, the cells were seeded onto a 6-well plate, and were counted every 2 days. This revealed that irradiated cells had a significantly lower proliferation rate than the control cells, and appeared to have stopped dividing altogether by day 15 post-irradiation (**Figure 2**).

To confirm what was happening at a molecular level, control and irradiated fibroblasts were seeded onto glass coverslips 10 days after irradiation, and stained for the proliferation marker Ki67 (**Figure 3a**). The percentage of Ki67 positive nuclei for control and irradiated HDFn was calculated, and it was found that irradiated cells express significantly less Ki67 than control (**Figure 3b**). However, a few Ki67 positive cells were still present following irradiation. To see whether this was due to the X-ray dose, further HDFn were treated with 20.44 Gy, 25.39 Gy, 30.35 Gy and 35.30 Gy and again stained for Ki67. Results revealed that following all X-ray doses, Ki67 positive cells were still present after 10 days (**Figure 3c**). As a result, it was decided to continue with a dose of 20.44 Gy for all future irradiation.

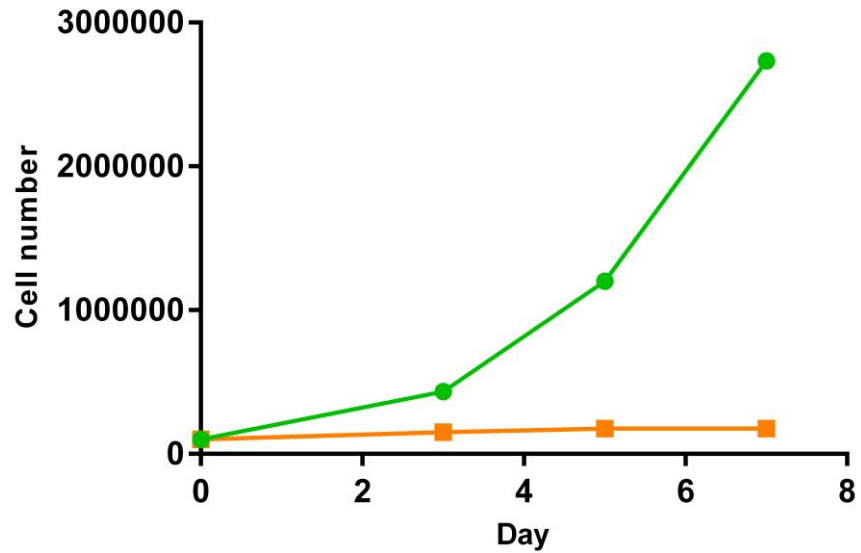


Figure 2: Change in cell proliferation after irradiation.

HDFn were irradiated with a dose of 20.44 Gy to induce premature senescence, and cultured under normal conditions for 10 days. Treated cells were then seeded onto a 6-well plate, alongside control HDFn and grown for 7 days. On days 3, 5 and 7, two wells were trypsinised and the cells were counted to assess proliferation. **Control**, **Irradiated**. Control HDFn proliferated rapidly across the 7 day period, whilst irradiated HDFn proliferated slowly until day 5 then stopped altogether. $n = 2$.

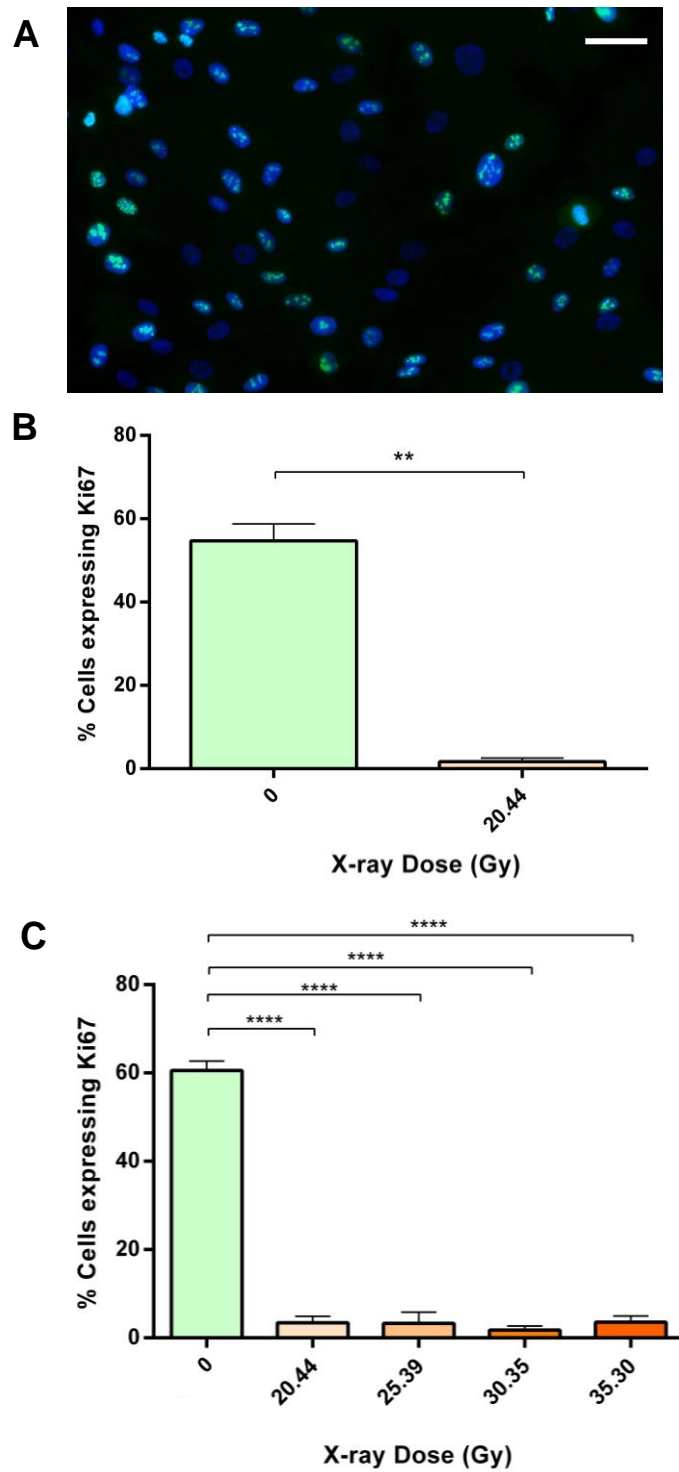


Figure 3: Analysis of Ki67 expression in control and irradiated HDFn

(A) HDFn were irradiated with a dose of 20.44 Gy to induce premature senescence. After 10 days, control and irradiated cells were seeded onto coverslips and stained for the proliferation marker Ki67 and the number of positively stained cells were counted. 100 cells

were counted for each condition. Scale bar = 50µm. (B) A paired two-tailed T-test revealed there was a statistically significant difference in the percentage of ki67 expressing cells following irradiation (** P ≤ 0.01, **** P ≤ 0.0001). (C) HDFn were irradiated with increasing X-ray doses to assess whether the percentage of Ki67 positive cells could be decreased. One-way ANOVA analysis revealed that there was no statistical difference between 20.44 Gy and higher doses of irradiation.

3.2 Identifying ageing biomarkers

Using the raw probe data obtained in P&G's MDE study, the individual probes for each gene of interest were isolated, and the general trends in dermal expression between the ages of 20 and 70 yrs were summarised (**Table 8**). Changes were observed in all of the selected markers. For the *in vitro* component of this study, irradiation-induced senescence and adult HDF obtained from photoexposed sites were used. Whilst P&G provided probe data from both arm and buttock biopsies, it was decided that it would be more relevant to focus on data obtained from arm biopsies only. According to the probe data, collagens I and IV decreased with age, as did the hyaluronic acid-producing enzyme, hyaluronan synthase 2. In conjunction with one another, MMP-1 expression was found to increase, whilst expression of TIMP-1 decreased. The cell cycle inhibitor p21 was increased with age, as were lamin A/C and the elastic fibres elastin and fibrillin 1



















Biomarker	Photoprotected	Photoexposed
Collagen I (alpha 1)		
Collagen IV (alpha 1)		
Elastin		
Fibrillin 1		
p21		
Lamin A/C		
Hyaluronan synthase 2		
MMP-1		
TIMP-1		

Table 8: Changes in ageing biomarker mRNA expression patterns in the dermis of young and old human skin samples

Raw probe data obtained from the P&G MDA study. Skin undergoes both intrinsic (photoprotected) and extrinsic ageing (photoexposed). Arrows indicate an increase or decrease in mRNA levels with age. Data is based on female donors in an age range of 20 yrs to 70 yrs .

3.3 Expression of ageing biomarkers in human skin

The final stage of the ageing biomarker analysis, was to see whether the changes observed in the TXP data matched with the protein levels in young and old human skin. Human skin samples were provided by P&G, and were taken from women aged in their 20s and 60s. For the purpose of this study, analysis was carried out on samples obtained from the arm; enabling a direct comparison with the *in vitro* work, which contained both irradiated HDFn, and HDF taken from photoexposed sites.

Initial H&E staining of the samples revealed clear changes in the appearances of young and old skin (**Figure 4**), such as alterations in dermal protein content, and appearance of the epidermis. The skin samples were then analysed via immunostaining, with sections being taken from three young and three old samples. Due to the time restraints of the project, it was only possible to optimise a limited number of antibodies for use on tissue sections, and as such the biomarkers assessed in the skin samples were elastin, collagen I, collagen IV and lamin A/C. Based on the TXP data, it was hypothesized that elastin and lamin A/C would increase with age, whilst collagen I and IV would decrease. Most of these predicted changes were observed; with the collagen content being lower in the old skin samples (**Figure 6 and 6**), and the number of disorganised elastin fibres increasing (**Figure 7**). However, lamin A/C was found to decrease rather than increase (**Figure 8**), which was more reminiscent of intrinsic ageing, rather than the extrinsic ageing associated with photoexposure.

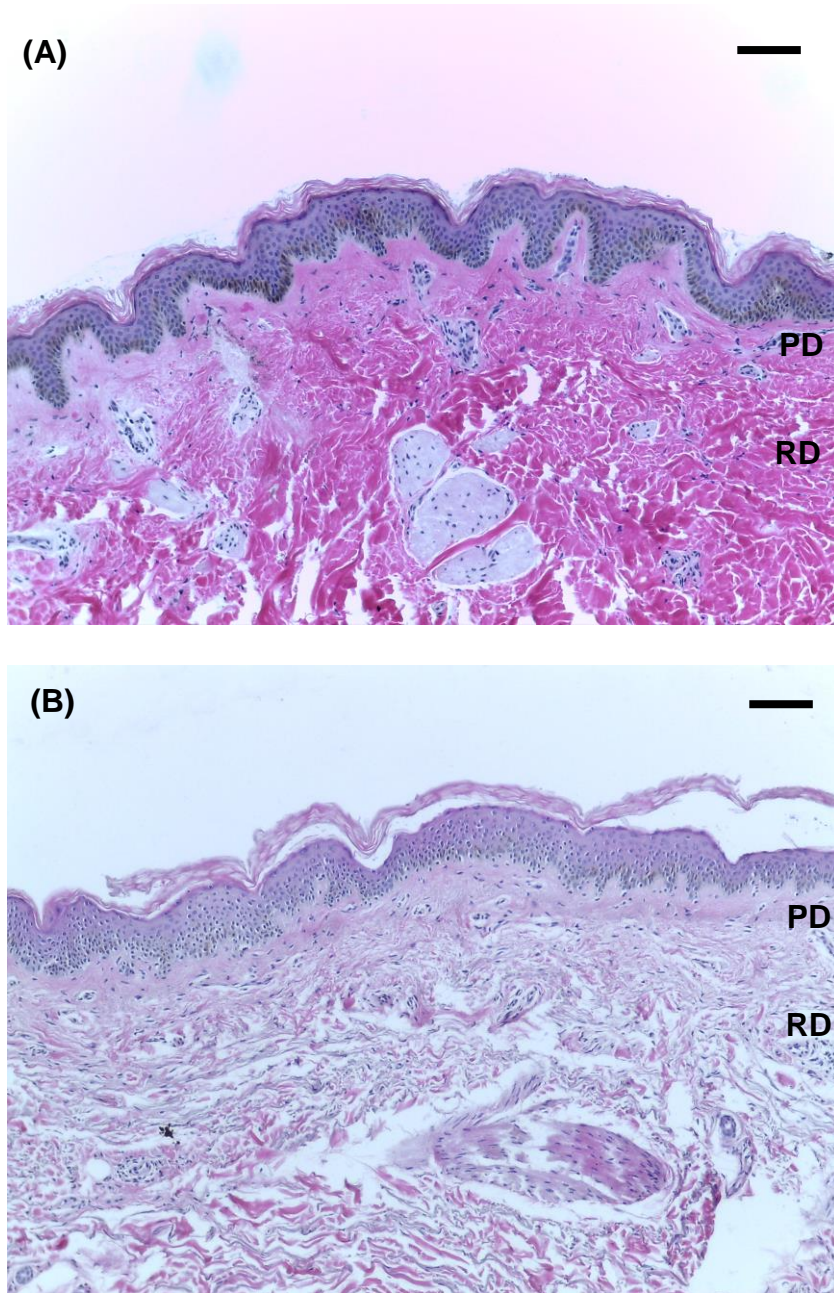


Figure 4: H&E stains of human skin samples taken from the arm biopsies of young and old donors.

Human skin samples taken from arm biopsies of female donors, provided by P&G. (A) Young skin showed extensive collagen expression throughout the entire dermis, indicated by the bright pink staining denoting high protein content. The epidermis is relatively thick, with distinctive rete ridges at the DEJ. (B) Old skin showed significant loss of collagen content, indicated by the pale staining in the dermal compartment. The epidermis appears thinner in some areas and there is clear loss of rete ridges. Scale bars = 100 μ m. PD = papillary dermis, RD = reticular dermis.

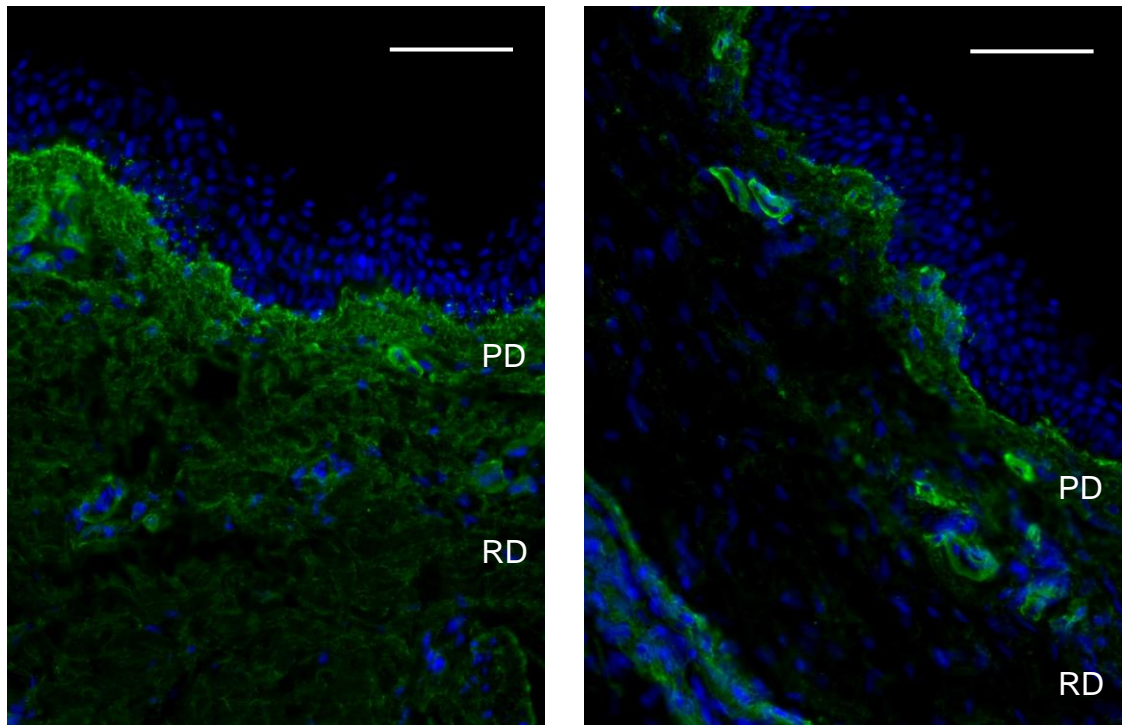


Figure 5: Immunofluorescence analysis of collagen I expression in young and old human skin samples

Human skin samples taken from arm biopsies of female donors, provided by P&G. OCT embedded sections fixed in PFA. Blue = DAPI, green = collagen I. (A) Young (21yrs) skin showed extensive collagen I expression throughout the entire dermis. (B) Old (63yrs) skin showed some collagen I staining in the papillary dermis, but the reticular dermis showed a significant loss of collagen fibres. Scale bars = 100 μ m. PD = papillary dermis, RD = reticular dermis. n = 3.

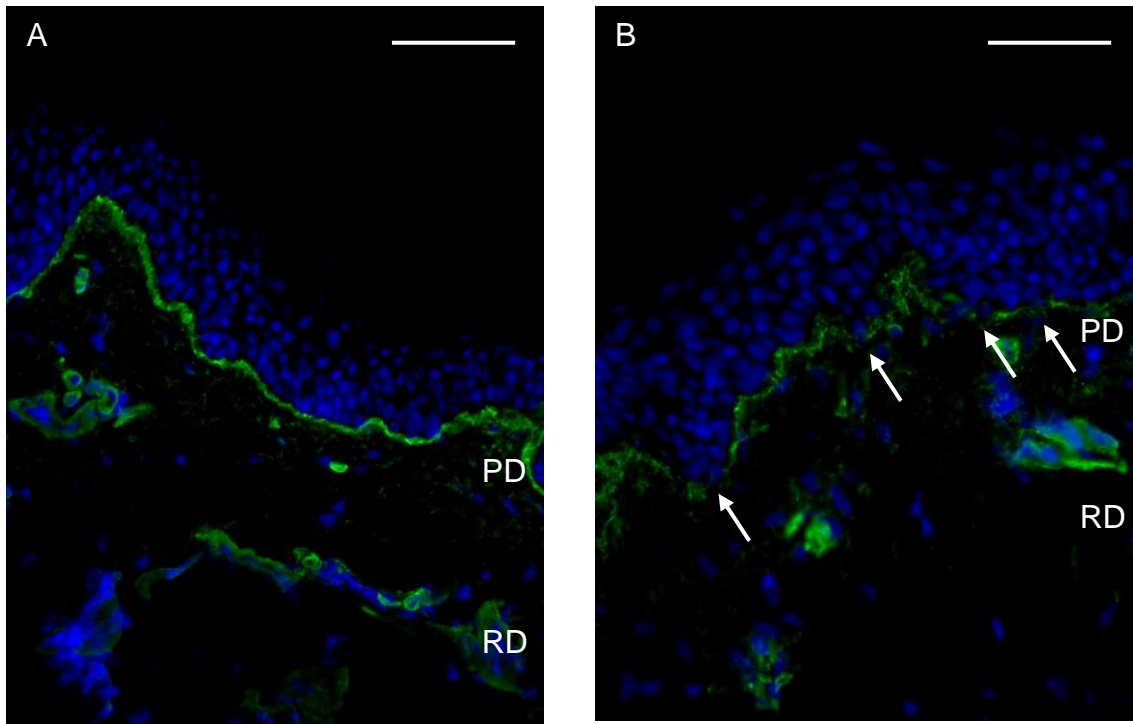


Figure 6: Immunofluorescence analysis of collagen IV expression in young and old human skin samples

Human skin samples taken from arm biopsies of female donors, provided by P&G. OCT embedded sections fixed in acetone. Blue = DAPI, green = collagen IV. (A) Young (21yrs) skin showed collagen IV expression along the entire epidermal basement membrane. (B) Old (65yrs) skin was found to have inconsistent, 'patchy' collagen V expression with some gaps (arrows). Scale bars = 100 μ m. PD = papillary dermis, RD = reticular dermis. n = 3.

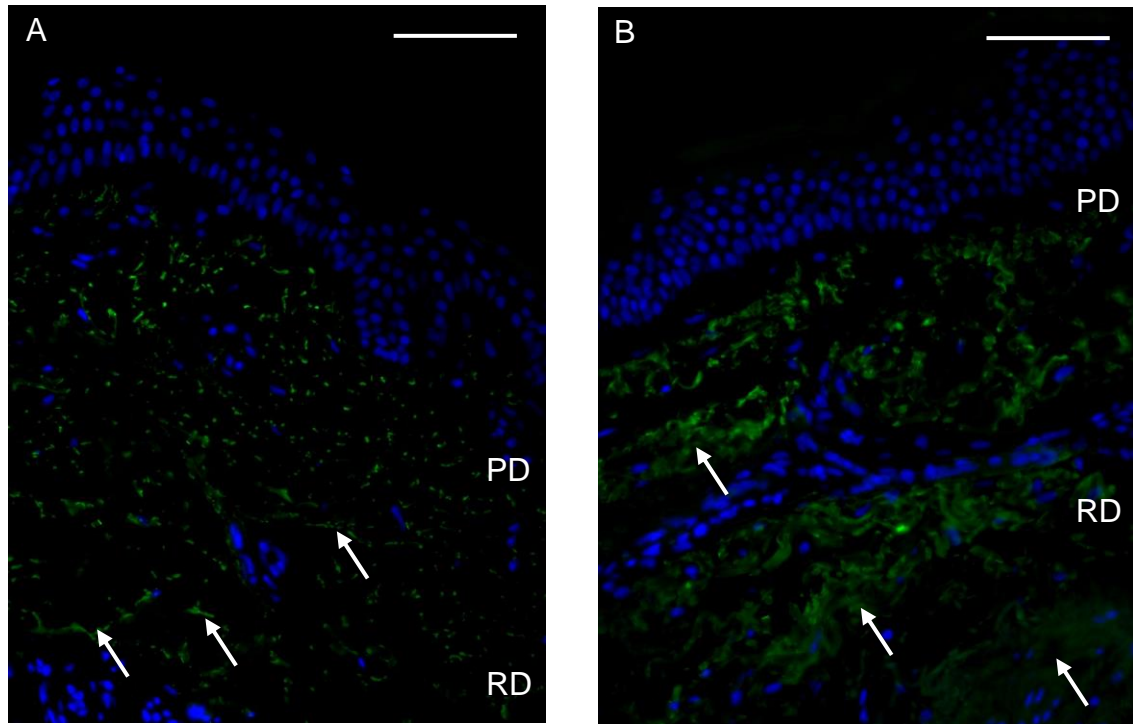


Figure 7: Immunofluorescence analysis of elastin expression in young and old human skin samples

Human skin samples taken from arm biopsies of female donors, provided by P&G. Paraffin embedded sections fixed in PFA. Blue = DAPI, green = elastin. (A) Young (21yrs) skin showed a moderate level of elastin fibre expression throughout the dermis, with some individual fibres visible (arrows). (B) Old (61yrs) skin was found to have a significantly greater proportion of elastin fibres, which formed disorganized aggregates in the dermis (arrows). Scale bars = 100 μ m. PD = papillary dermis, RD = reticular dermis.

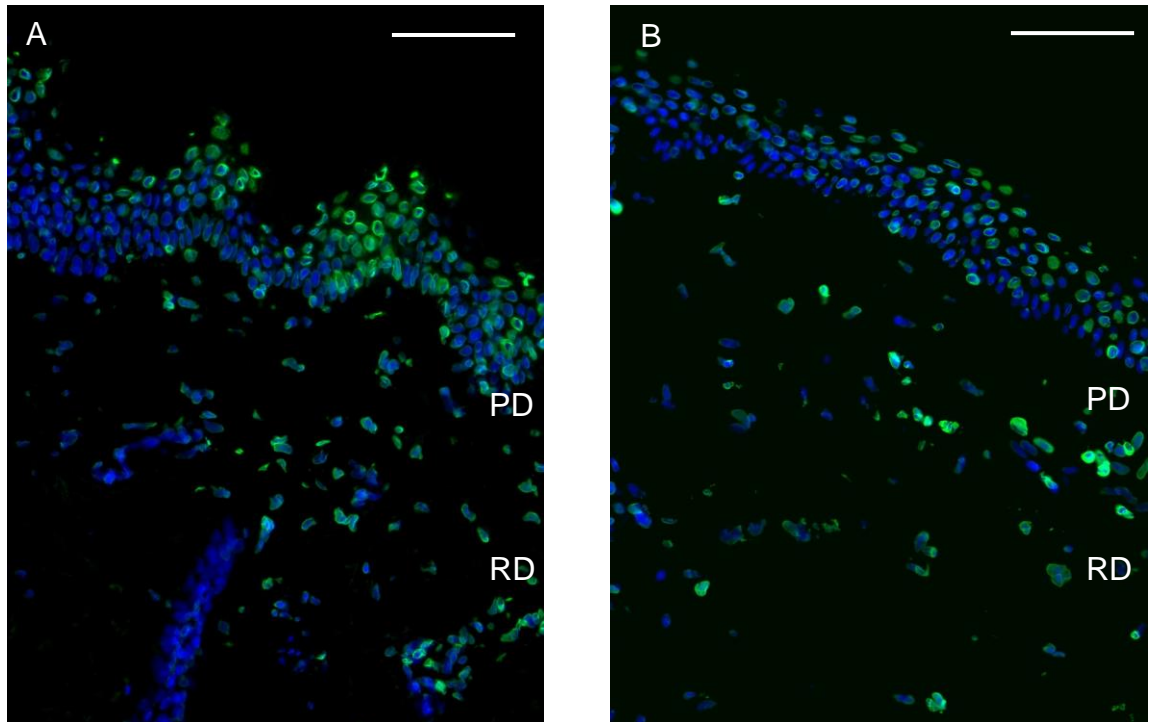


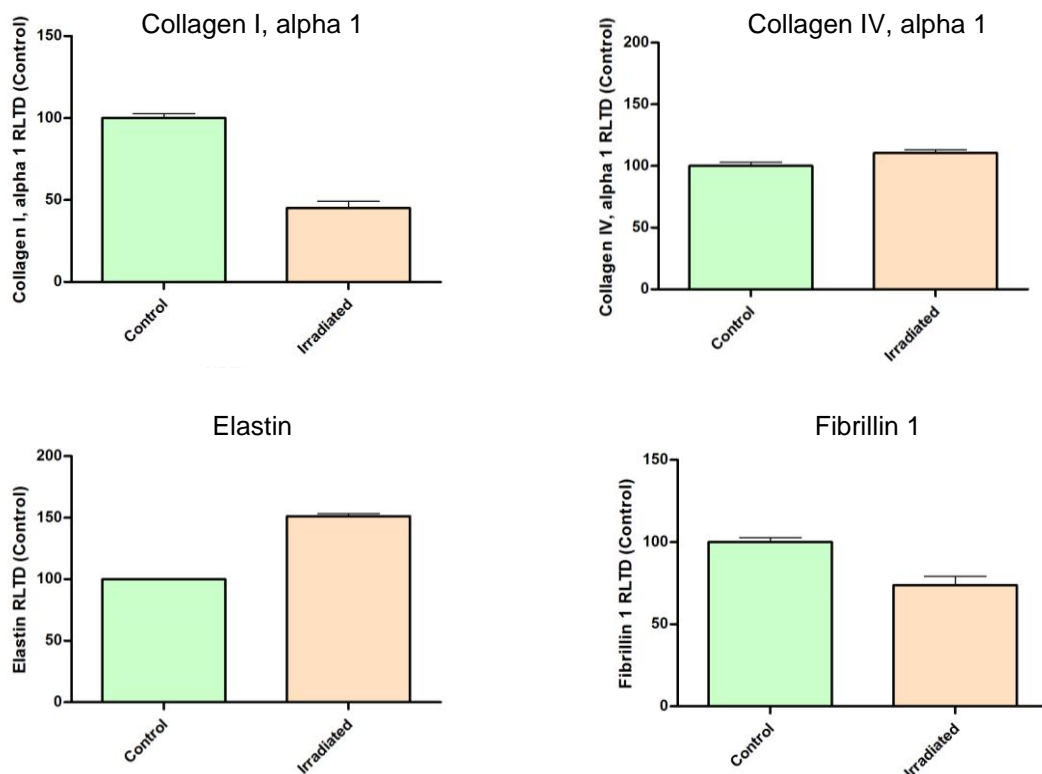
Figure 8: Immunofluorescence analysis of lamin A/C expression in young and old human skin samples

Human skin samples taken from arm biopsies of female donors, provided by P&G. OCT embedded sections fixed in PFA. Blue = DAPI, green = lamin A/C. (A) Young (21yrs) skin showed strong lamin A/C staining in the epidermis; particularly in the suprabasal layers. (B) Old (61yrs) again showed mainly suprabasal staining, but there appeared to be less than was observed in the young skin. Scale bars = 100 μ m. PD = papillary dermis, RD = reticular dermis. n = 3.

3.4 Ageing biomarkers in irradiation-induced senescent HDFn

3.4.1 Changes in gene expression

In order to assess gene expression levels of the identified biomarkers, qPCR analysis was carried out. RNA lysates were generated from control and irradiated HDFn, 10 days after irradiation treatment. qPCR analysis was carried out, using TaqMan primers for biomarkers selected from P&G's transcriptomic (TXP) data. Consistent with literature on extrinsic age-related changes, it was observed that collagen I decreased following irradiation, whilst elastin and hyaluronan synthase 2 increased. However, fibrillin 1 expression was observed to decrease, as seen in intrinsic ageing. Moreover, MMP-1 expression decreased, and TIMP-1 and collagen IV increased (**Figure 9**); all changes that are not observed in either intrinsic or extrinsic ageing of skin.



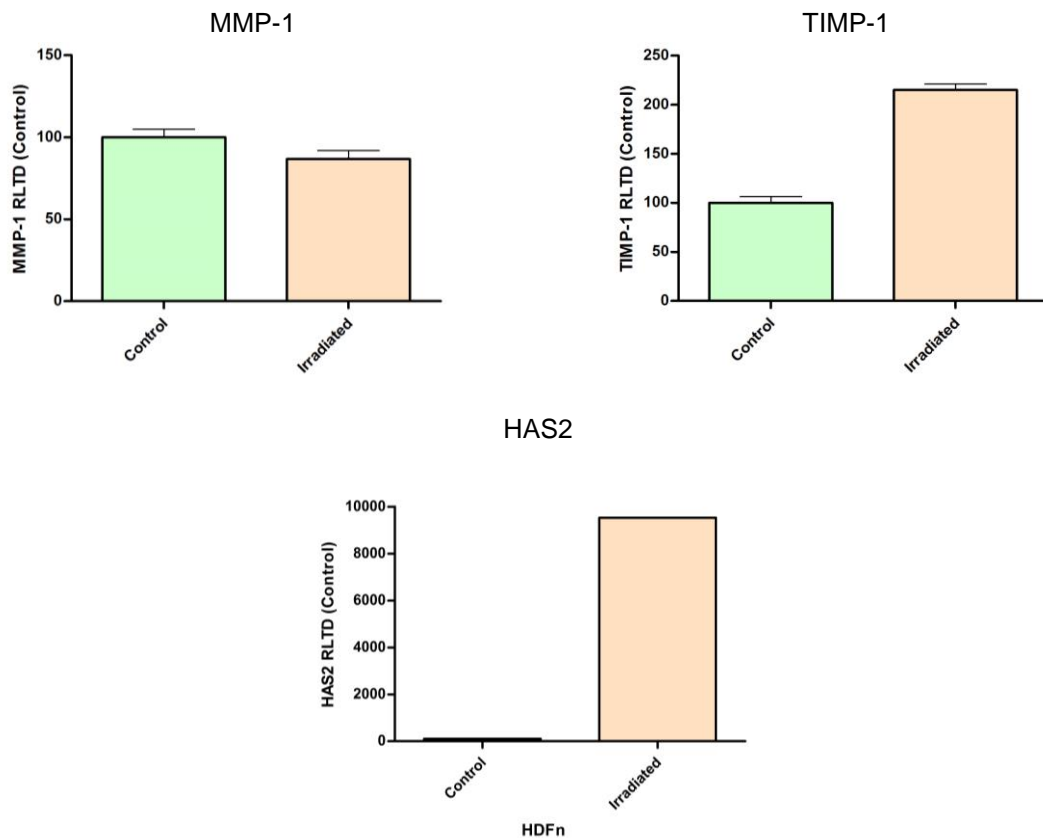


Figure 9: qPCR analysis of biomarker expression in control and irradiated HDFn

The average ΔCt of irradiated HDFn was normalised to that of the control HDFn using the equation $1/\text{POWER}(2, \text{ave}\Delta Ct^x - \text{ave}\Delta Ct^y)$. The Ct value was used to calculate the relative transcriptional difference compared to control HDFn (RLTD (control)). Error bars represent the standard error of the mean (SEM). Variations in the gene expression of some key biomarkers, appear to suggest that irradiation does induce several age-related changes.

3.4.2 Changes in protein levels

Protein was extracted from whole cell lysates 10 days after irradiation, and analysed by Western blot. Elastin and collagen I behaved as observed in the qPCR analysis. In addition, p21 and p16 levels increased following irradiation; consistent with reports in the literature. Lamin A/C was expected to increase, based on the data from P&G's microarray analysis. However, lamin C was observed to decrease, and lamin A was entirely absent in irradiated HDFn (**Figure 10**).

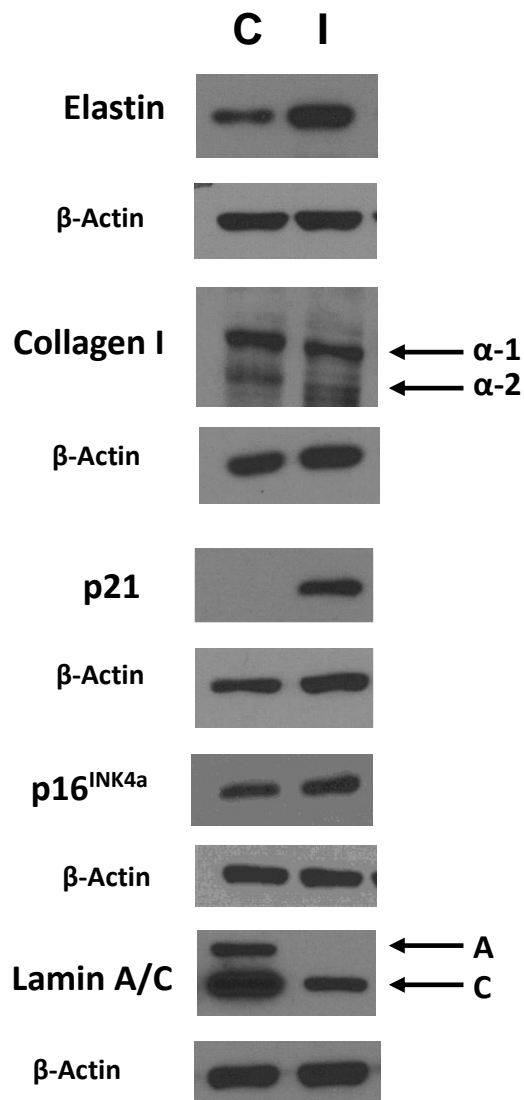


Figure 10: Western blot analysis of biomarker expression in control and irradiated HDFn

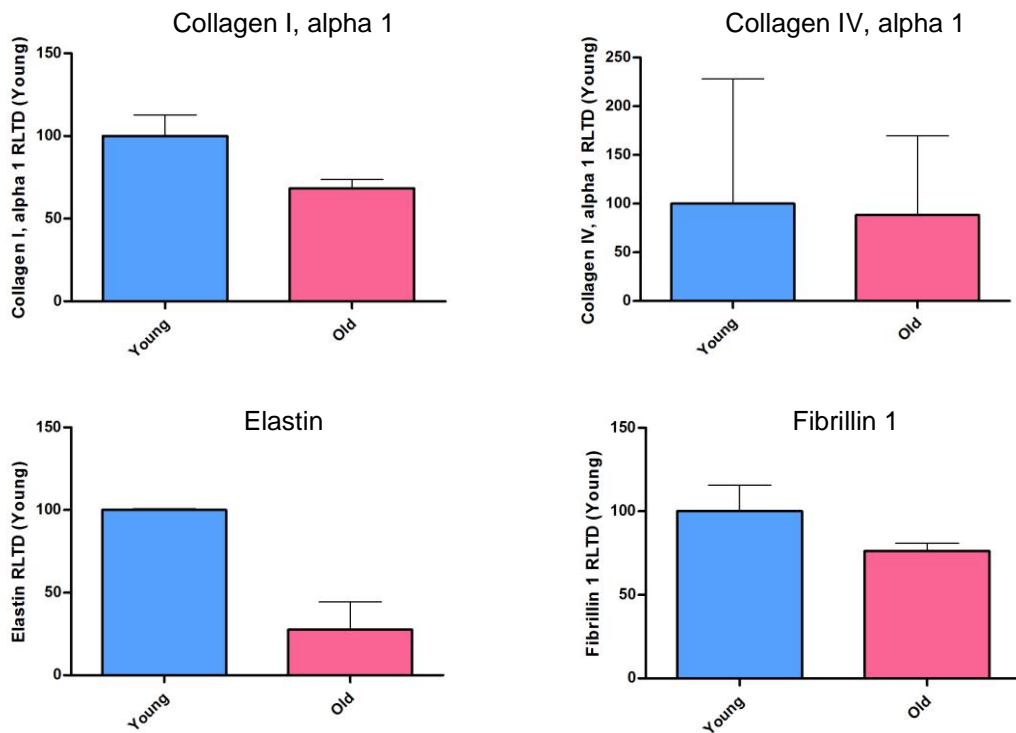
20µg of protein from each lysate was run through a gel at 120V, and transferred at 250mA. Blocking was done in 5% milk, and β-actin was used as a loading control. Results suggest that irradiation does induce an ageing phenotype in HDFn. Changes observed in elastin, collagen I, p21 and p16 follow observations from the literature. The total loss of lamin A in irradiated cells was unexpected. Elastin = 68 kDa , collagen I = 139 kDa, (α-1) 129 kDa (α-2), p21 = 18 kDa, p16^{INK4a} = 17 kDa, lamin A/C = 74 kDa.

3.5 Ageing biomarkers in young and old HDF

The cells were obtained from the Coriell Institute Biorepository, with three cell lines for young, and three for old; all obtained from photoexposed biopsy sites. As a result, it was hypothesized that the cells would exhibit changes in biomarkers associated with extrinsic ageing.

3.5.1 Changes in gene expression

In order to provide a more *in vivo*-like experimental group, HDF taken from young and old donors were also analysed. ‘Young’ cell lines were taken from donors aged 10 to 12yrs, and ‘old’ cell lines were taken from donors aged 82yrs. All donors were male, and the majority came from biopsies of the arm. Changes in gene expression between the cell lines were analysed using qPCR. Due to problems with RNA extraction, only two cell lines from each age group were used; GM03348 and GM00323 (young) and AG12443 and AG11651 (old) (**Figure 11**). qPCR analysis was carried out, using TaqMan primers for biomarkers selected from P&G’s transcriptomic (TXP) data. Changes observed in elastin, fibrillin 1 and hyaluronan synthase 2 do not match those associated with extrinsic ageing in the literature.



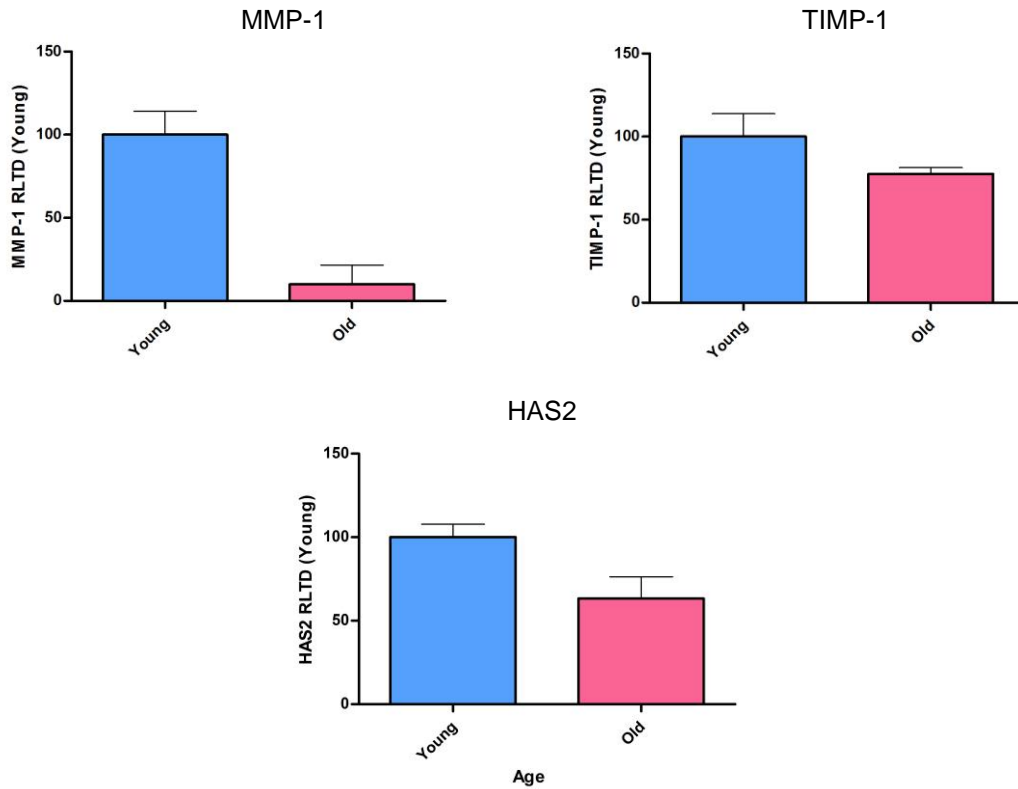


Figure 11: qPCR analysis of biomarker expression in young and old HDF

The average ΔCt of old HDF was normalised to that of the young HDF using the equation $1/POWER(2, ave\Delta Ct^x - ave\Delta Ct^y)$. The Ct value was used to calculate the relative transcriptional difference compared to young HDF (RLTD (young)). Error bars represent the standard error of the mean (SEM). Changes were observed between young and old HDF for all biomarkers analysed. However, the changes reflected those seen in intrinsic ageing rather than extrinsic. The decrease observed in MMP-1 with age, does not reflect any known ageing phenotype.

3.5.2 Changes in protein levels

Western blots were used to analyse changes in protein levels between young and old HDF. Protein was extracted from whole cell lysates and a selection of biomarkers were assessed, based on those able to be optimised in the time frame of the project. Changes in protein level were a little harder to decipher than with the HDFn, due to wide variation between the cell lines. Cell cycle inhibitor, p21 was not found to be present in either the young or old cells. Moreover, Lamin A/C was so variable, that it was not possible to conclude if there was a change with age. Elastin

levels did appear to decrease with age, which coincided with the data obtained for gene expression. In addition, collagen I also seemed to decrease, though most cell lines did not produce a band for the α -1 chain, so this could not be directly compared to the qPCR analysis (**Figure 12**).

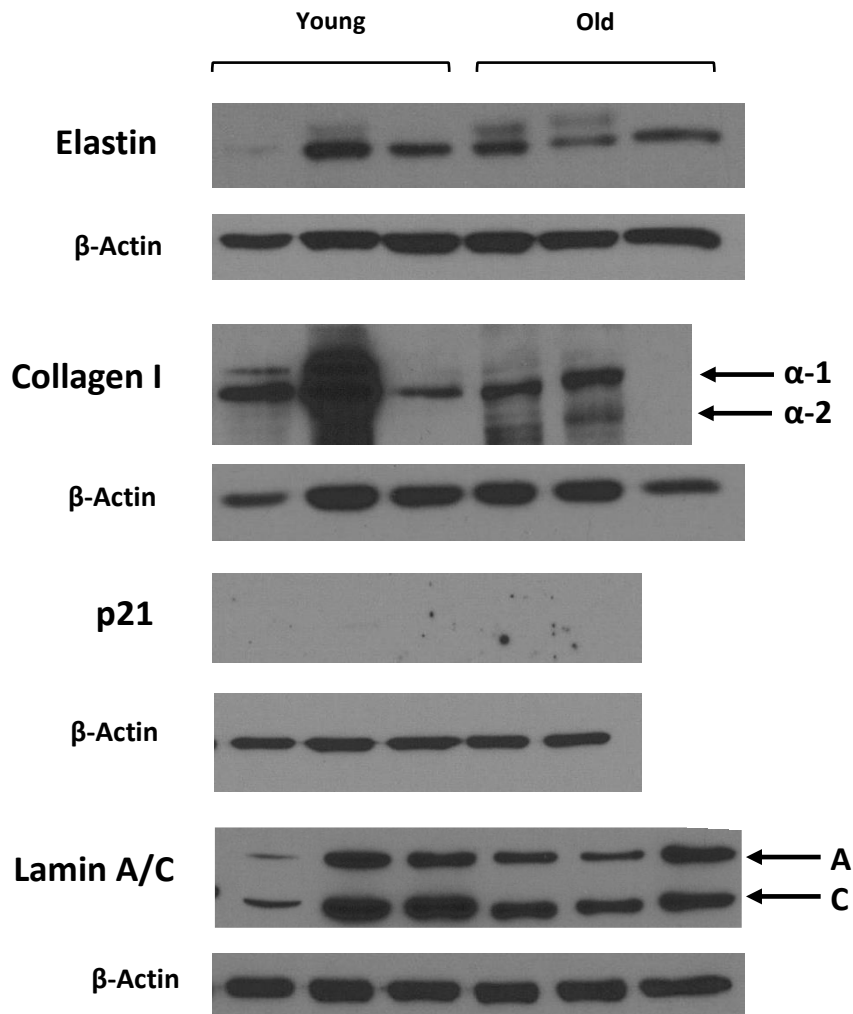


Figure 12: Western blot analysis of biomarker expression in young and old HDF

20 μ g of protein from each lysate was run through a gel at 120V, and transferred at 250mA. Blocking was done in 5% milk, and β -actin was used as a loading control. Results are rather ambiguous at first glance due to clear variation amongst different cell lines. It appears that old HDF possessed a slightly decreased level of elastin and collagen I. However, p21 and lamin A/C appeared to show no change between young and old cells. Arrows show labelling where two bands are expected to be seen. Elastin = 68 kDa, collagen I = 139 kDa, (α -1) 129 kDa (α -2), p21 = 18 kDa, lamin A/C = 74 kDa.

3.6 Progerin expression in HDF

3.6.1 Nuclear circularity and abnormality

Progerin is a truncated form of lamin A/C that is associated with accelerated ageing diseases, such as Hutchinson-Gilford Progeria Syndrome. Abnormalities of the nuclear envelope have been associated with progerin expression as the nuclear scaffold becomes compromised. Consequently, the presence of nuclear abnormalities was assessed in control and irradiated HDFn and young and old HDF. Cells were seeded onto 12mm coverslips, and immunostained for lamin A/C which highlights the nuclear envelope. Two techniques were then used to assess abnormalities: calculating the nuclear circularity, and counting the number of abnormalities visible to the naked eye. Circularity was calculated using the computer program Image J, which utilises the equation $4\pi \times \text{area}/\text{perimeter}^2$, giving a circle a value of 1.0. The nuclear circularity of 100 cells for each group was calculated, and the average used to plot graphs (**Figure 13** and **Figure 14**). Visible abnormalities were assessed by eye (**Figure 15**), with the percentage calculated from number of abnormal nuclei in 100 cells, for each group. The results for nuclear circularity did not follow the predicted pattern of irradiation/age inducing decreased circularity. However, visible abnormalities did show a positive trend with irradiation and age, despite not being statistically significant.

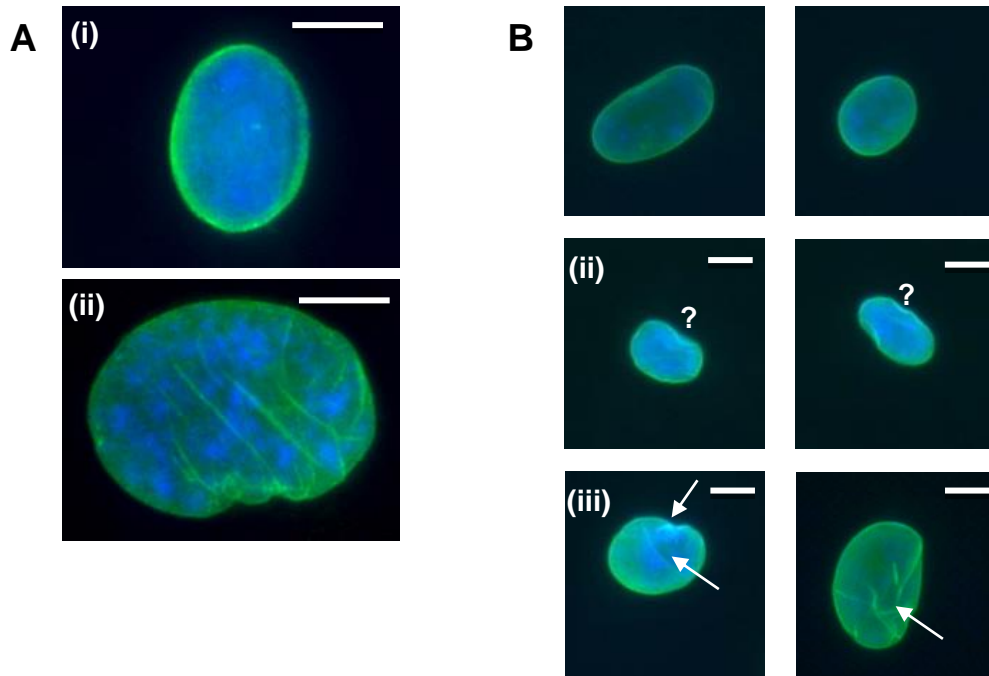


Figure 13: Lamin A/C staining revealed abnormalities in the nuclear envelope

Cells were seeded onto 12mm coverslips and immunostained using an anti lamin A/C antibody and mounted with VECTASHIELD® containing the DNA stain DAPI. Above images show nuclei from control and irradiated HDFn. Scale bars = 10µm. DAPI = blue, lamin A/C = green. (A) (i) Untreated HDFn had mostly 'normal' nuclei, with the nuclear envelopes appearing to have a smooth surface. (ii) Irradiation of HDFn appeared to result in an increase in the number of 'abnormal' nuclei. These were characterised by invaginations and creases in the nuclear envelope. (B) Number of abnormalities was assessed visually: (i) nuclei with completely smooth edges and no apparent creases were labelled 'normal', (ii) nuclei where changes were only minor (?) were also labelled 'normal', (iii) nuclei with clear invaginations and creases (**arrows**) were labelled 'abnormal'.

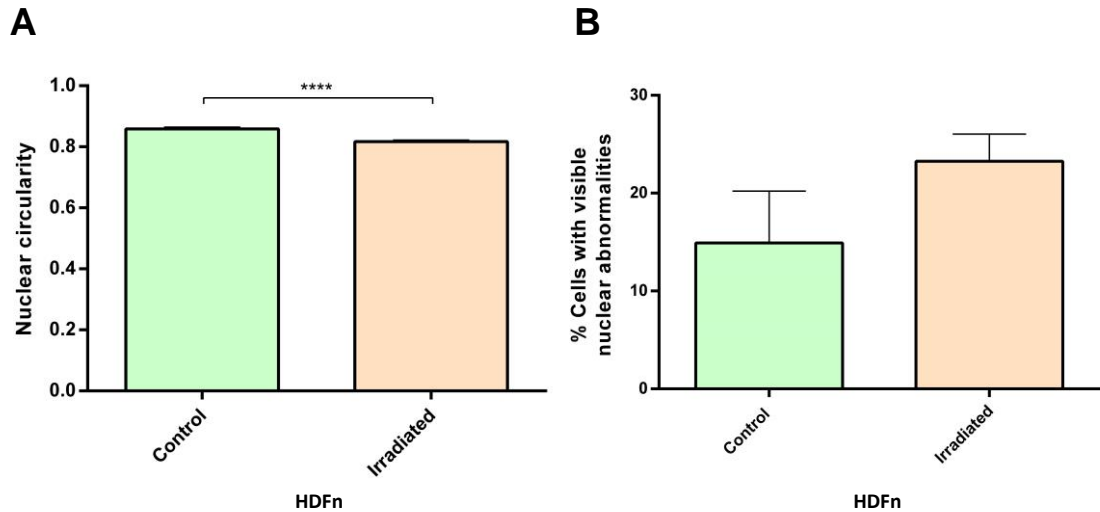
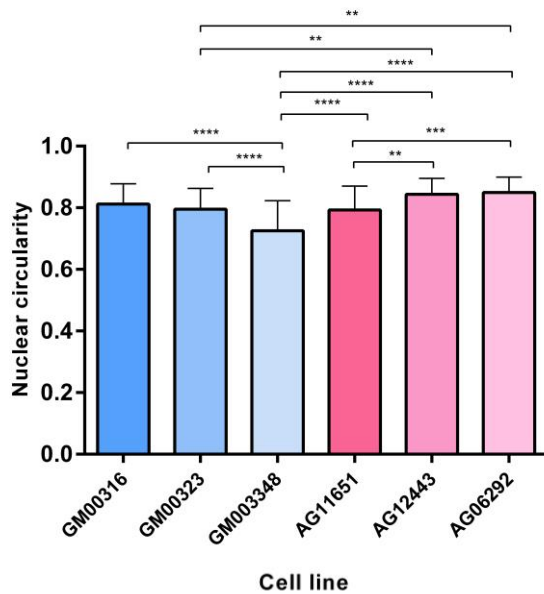
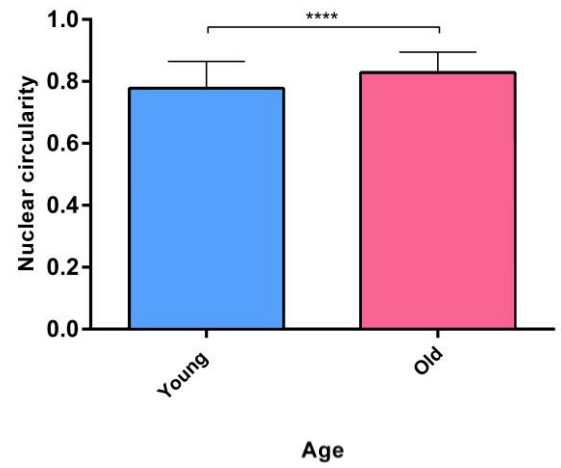
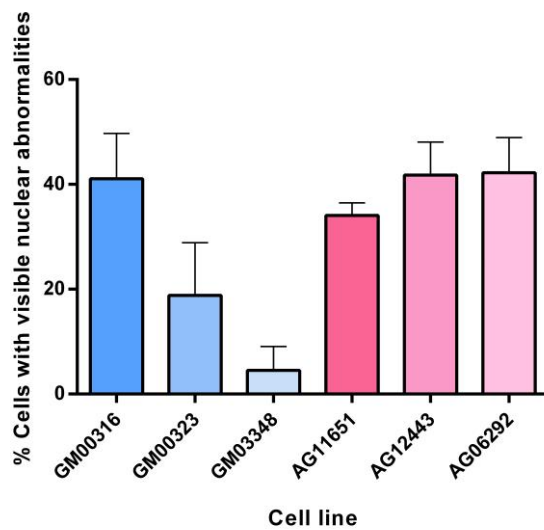
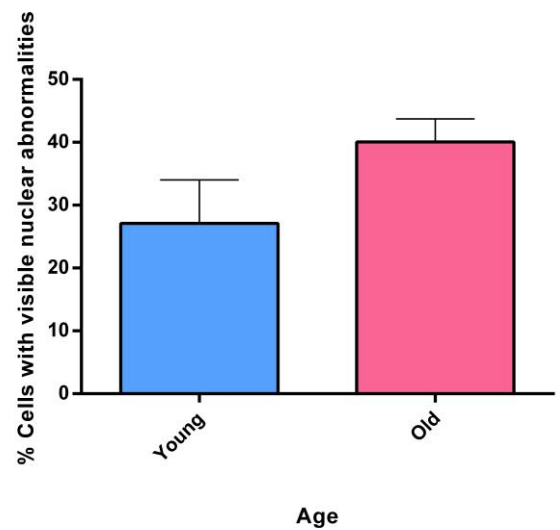


Figure 14: Nuclear circularity and visible abnormality analysis for control and irradiated HDFn

HDFn were treated with an irradiation dose of 20.44Gy and cultured for 10 days before being seeded onto 12mm coverslips, alongside untreated HDFn. Cells were immunostained using an anti lamin A/C antibody and mounted with VECTASHIELD® containing the DNA stain DAPI. (A) ImageJ was used to calculate nuclear circularity using the equation $4\pi \times \text{area}/\text{perimeter}^2$, with a circle being given the value of 1.0. Observed a statistically significant increase in circularity after irradiation (**** $P \leq 0.0001$). (B) Nuclei were visually assessed for abnormalities, as specified in **Figure 12**, and the percentage was calculated. Abnormalities were observed to increase after irradiation, but this was not a significant change.

A (i)**A (ii)****B (i)****B (ii)****Figure 15:** Nuclear circularity and visible abnormality analysis of young and old HDF

HDF taken from young (10 – 12yrs) and old (81yrs) donors were compared. Cells were seeded onto 12mm coverslips and immunostained using an anti lamin A/C antibody and mounted with VECTASHIELD® containing the DNA stain DAPI. (A) ImageJ was used to calculate nuclear circularity using the equation $4\pi \times \text{area}/\text{perimeter}^2$, with a circle being given the value of 1.0. Nuclear circularity was observed to increase with age, with statistical significance (** $P \leq 0.01$, *** $P \leq 0.001$, **** $P \leq 0.0001$). (B) Nuclei were visually assessed

for abnormalities, as specified in **Figure 13**, and the percentage was calculated. Abnormalities were also observed to increase with age, but this was not significant.

3.6.2 Progerin protein levels

Western blot analysis of the control and irradiated HDFn, and young and old HDF was carried out to assess protein levels of progerin. Protein was extracted from whole cell lysates, and progerin levels were analysed. The breast cancer cell line MDA-MB-231 was used as a positive control, as it has been shown to express the truncated form of lamin A (Tang *et al.*, 2010). However, whilst results showed that progerin was expressed in all of the cells used, there appeared to be no correlation between irradiation or age, and level of protein (**Figure 16**). Moreover, each technical and biological repeat produced a different result, further cementing the lack of a correlation.

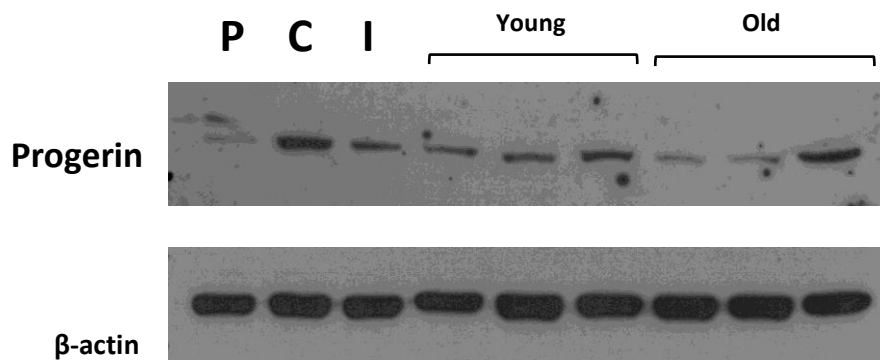


Figure 16: Western blot analysis of progerin expression in HDF

Protein lysates were generated from control and irradiated HDFn, and young and old HDF. 20µg of protein from each lysate was run through a gel at 120V, and transferred at 250mA. Blocking was done in 5% milk, and β-actin was used as a loading control. P = positive control (MDA-MB-231), C = control HDFn, I = irradiated HDFn. The bands observed clearly show that there is no apparent correlation between irradiation or age, and level of progerin protein. Progerin = 70 kDa.

3.7 Ageing biomarkers in irradiation-induced senescent HDFn grown on a 3D Alvetex® scaffold

To compare ageing biomarkers in 2D cultured cells with those grown in a more '*in vivo*-like' environment, HDFn were grown on an Alvetex® for 28 days. Half of the cells were then irradiated with a dose of 20.44 Gy and cultured for a further 10 days. Lysates were then obtained from the cells, and Western blot was used to assess the marker of interest. The results were found to be similar to those seen in the 2D analysis, though collagen I produced only one band, that was heavier than both alpha 1 and alpha 2; potentially making it a dimer. Following irradiation, the band appeared stronger; contrary to expectations (**Figure 17**)

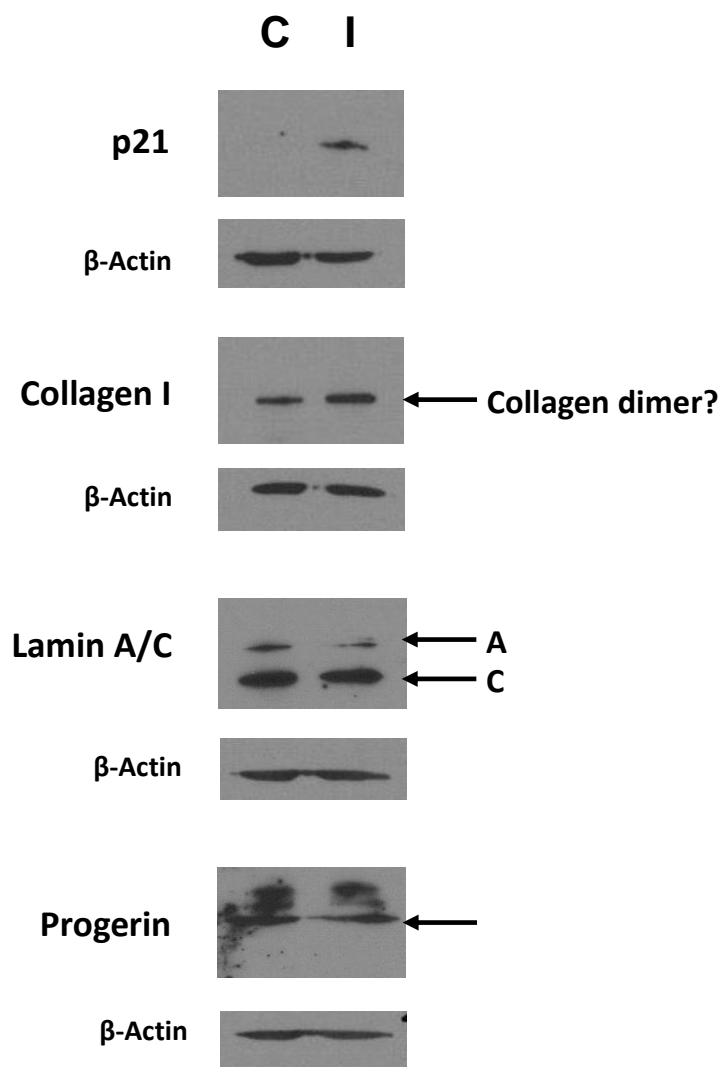


Figure 17: Western blot analysis of ageing biomarker expression in control and irradiated HDFn grown on a 3D Alvetex® scaffold

20µg of protein from each lysate was run through a gel at 120V, and transferred at 250mA. Blocking was done in 5% milk, and β-actin was used as a loading control. As observed in the 2D analysis, irradiation induced expression of p21, and a decrease in expression of lamin A. Instead of the alpha 1 and 2 chains being visible, only one band was visible for collagen I. At ~250 kDa, this could be a collagen I dimer, and it appeared to increase following irradiation; contradictory to the hypothesis. Progerin once again showed no correlation between irradiation and protein level. p21 = 18 kDa, collagen I = 139 kDa, (α-1) 129 kDa (α-2), lamin A/C = 74 kDa, progerin = 70 kDa.

4. Discussion

Ageing biomarkers are a vital component of the skin ageing process. It is changes in the expression and degradation of these proteins that are responsible for the familiar phenotypes of aged skin such as loss of elasticity, wrinkling, drying and increased fragility. Gene expression analysis of human skin, has enabled the identification of key biomarkers involved in the ageing process. These data have been compared with immunofluorescence analysis of human skin samples; as well as used to examine the behaviour of cells *in vitro*, with the aim of creating an aged skin model that mimics tissue as closely as possible.

In this investigation, comparisons were made between three different experimental groups. HDFn were irradiated to induce a senescent phenotype, and thus compared to untreated HDFn to provide an *in vitro* model of young versus old fibroblasts. In addition, cells obtained from the Coriell Institute were also analysed; with three 'young' and three 'old' cell lines being used in the comparisons. Finally, human tissue samples provided by P&G enabled *in vitro* findings to be directly evaluated alongside human skin samples taken from young and old donors. The aim of this was to determine the best technique to be used in the future development of an *in vitro* aged skin model that is as physiologically relevant as possible.

4.1 HDFn irradiated and then cultured for 10 days still expressed Ki67

Ki67 is a proliferation marker that was used to assess the proliferative capacity of HDFn, before and after treatment with an X-ray dose of 20 Gy. A key feature of senescence is irreversible cell cycle arrest (Leontieva *et al.*, 2010), and thus, in order to say that irradiated HDFn have a senescent phenotype, the cells must not be proliferating. Irradiation has been shown to cause cell cycle arrest in previous studies, (Dalle Pezze *et al.*, 2014) and indeed in this study, X-ray treatment significantly decreased the expression of Ki67. However, following all treatment doses, a small percentage of HDFn still stained positive for Ki67 (**Figure 3c**). A simple explanation for this, is that perhaps 10 days is not a long enough period for every cell to stop proliferating. Looking at the graph in **Figure 2**, the number of irradiated HDFn was still increasing up until day 5; suggesting that if Ki67 staining

had been carried out 15 days after X-ray treatment, the cells might no longer have been expressing it.

In addition, on examination of the images taken from the Ki67 stained HDFn, it is clear that some of the staining is abnormal. Ki67 is expected appear as foci within the cell nucleus (**Figure 3a**); but some of the staining observed in the irradiated cells showed presence of the protein outside of the nucleus, with the foci appearing irregular (**Figure 18**). Ki67 is known to be expressed in the late G1, and all of the S and G2 phases of the cell cycle; with its peak being during mitosis, before it is rapidly degraded (Wu *et al.*, 2000). Irradiation induces p53-mediated G1 arrest (Agami & Bernards, 2000), and thus it is possible that the cells found to contain abnormal Ki67 localisation were fixed whilst they were exiting the M-phase, and still degrading Ki67. This could explain the abnormal distribution and appearance of the protein in the immunofluorescent analysis. Whilst an explanation for cytoplasmic Ki67 has yet to be found (Faratian *et al.*, 2009), it is observed in some cancers, and has been seen both in tissue and *in vitro*; suggesting a functional explanation. If the theory of degradation is correct, this further supports the idea that, had the cells been fixed several days later, the immunofluorescent analysis might have revealed the total loss of Ki67 that was initially expected. Nonetheless, as the percentage of Ki67 positive cells was less than 5% following irradiation, their presence was not deemed significant enough to have had any impact on the results obtained. As a result, we are satisfied that an X-ray dose of 20 Gy is sufficient to produce a reliable, and replicable senescent-phenotype in HDFn.

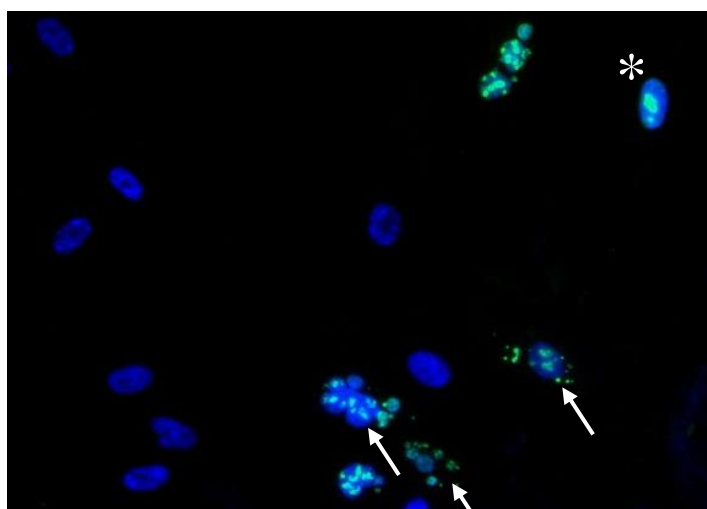


Figure 18: Changes in Ki67 expression in irradiated HDFn

HDFn were irradiated with a dose of 20 Gy, then cultured for 10 days. Cells were then fixed and immunostained with an anti-Ki67 antibody. Ki67 usually appears as foci in the nucleus (*). However, some cells appeared to contain a large number of smaller foci, with some appearing in the cytoplasm (arrows).

4.2 Changes in ageing biomarkers in irradiated HDFn differed from photoexposed TXP results

4.2.1 Gene expression changes of ageing biomarkers

From the TXP data provided by P&G, we were able to isolate a selection of ageing biomarkers to analyse; enabling us to assess whether irradiated HDFn truly mirrored the behaviour of 'old' cells. The first point of analysis was to see what was happening to the cells at a genetic level. As irradiation is a similar stress to UV exposure in terms of the DNA damage response, it was hypothesized that irradiated HDFn would follow a pattern of extrinsic ageing. However, it was observed that, whilst some gene responses were similar to those found in extrinsic tissue, others were more reminiscent of intrinsic ageing, and a couple did not match any ageing process at all.

It is well documented in the literature, that ageing leads to the gradual degradation of collagens. This was observed in the TXP data; with both collagens I and IV decreasing in photoexposed skin. However, following irradiation, it was found that collagen IV expression increased slightly in HDFn, which is contradictory to the majority of irradiation studies (Hee Lee *et al.*, 2004). However, investigations into the effects of radiation on tumours, have observed that collagens I, III and IV can increase in the first 24 hours, and even continue increasing for up to 14 days following irradiation (Znati *et al.*, 2003 and Finkelstein *et al.*, 1994). As a result, this could potentially explain why collagen IV expression was slightly elevated 10 days after irradiation treatment. Nevertheless, the more likely reason for this result is that the HDFn were cultured in a 2D environment. Collagen IV is the key component of the epidermal basement membrane; a structure for which fibroblasts grown in a plastic culture flask have no requirement. As such, it is likely that the gene expression of collagen IV in both control and irradiated HDFn, does not truly reflect the behaviour of the cells as it would be *in vivo*.

Another discrepancy in the HDFn qPCR results, is the expression of elastin and fibrillin 1. In the TXP analysis, both proteins were found to increase with exposure to UV radiation. Moreover, this is well documented in the literature; photoexposure leading to solar elastosis due to an increase in elastin and fibrillin expression (Park *et al.*, 2010). In the results obtained from the HDFn analysis, it was found that elastin expression increased following irradiation, whilst fibrillin 1 decreased. *In vivo*, fibrillin-rich microfibrils co-localise with elastin fibres, and form a sheath around them; meaning that expression of both proteins usually correlates with the other (Naylor *et al.*, 2011). The most likely explanation for the unusual observation in our results, is that the cells were cultured in a 2D environment. *In vivo*, the ECM plays a key role in providing mechanical stimulus to the cell; ultimately leading to control of gene expression by triggering internal pathways (Wu *et al.*, 2011). When cells are cultured in a flask, the external stimuli are drastically different from the environment within a tissue; resulting in perturbation of gene expression within the cells (Birgersdotter *et al.*, 2005). As such, had the HDFn been grown in a 3D environment, for example by using an Alvetex[®] scaffold, the qPCR results may have followed the predicted pattern associated with extrinsic ageing. Moreover, it is important to remember that qPCR only provides us with information on the mRNA levels; which does not necessarily reflect the amount of protein present within the cells (Koussounadis *et al.*, 2015).

In addition to the elastic fibres, MMP-1 and TIMP-1 also failed to follow the gene expression patterns associated with ageing; this time both intrinsic and extrinsic. It is well characterised that MMP-1 increases with age as a result of the build of ROS (Masaki, 2010). As TIMPs inhibit the behaviour of MMPs, a decrease in TIMP expression is also associated with ageing; the combination of both contributing to the increase in collagen degradation observed in both photoprotected and photoexposed ageing (Fisher *et al.*, 2014). However, in the qPCR results, it was observed that following irradiation, HDFn expressed a decreased amount of MMP-1 and a significantly increased amount of TIMP-1. Once again, a feasible explanation is that gene expression could have been altered as a result of the unnatural external environment provided by plastic cultureware (Edmondson *et al.*, 2014). However, X-ray radiation is not a natural source of stress, and so we cannot assume that it will trigger changes that entirely mimic UV exposure. A study by Yavas *et al.* (2014), looked at the effects of radiation on human gingival fibroblasts, and observed that a dose of as low as 6 Gy was enough to induce an increase in TIMP-1 mRNA levels. Moreover, in a study on rectal cancer patients receiving radiotherapy, Angenete *et*

al. (2009) observed that irradiation had no effect on the mRNA levels of MMP-1; though they did see an increase in other MMPs. Consequently, the unusual mRNA changes witnessed in HDFn following irradiation, could be due to the fact that cells respond differently to exposure to UV radiation, and X-ray radiation.

The final gene of interest that did not match the TXP data, was *HAS2*. Hyaluronan synthase 2 is a membrane bound enzyme that produces the ECM component hyaluronan (HA) (Siiskonen *et al.*, 2015). In the P&G TXP data, *HAS2* mRNA levels decreased in both photoprotected and photoexposed skin, so on this basis it was hypothesized that the HDFn qPCR results would reveal a decrease following irradiation. However, instead HDFn were observed to produce a significantly greater amount of *HAS2* mRNA after X-ray treatment. Whilst this contradicts the TXP results, in the literature it is well documented that dermal HA increases in response to UV exposure (Naylor *et al.*, 2011). It has been found that exposing nude mice to UV radiation, for as short a period as 5 minutes, is enough to induce an increase in HA synthesis (Papakonstantinou, 2012). However, chronic UV exposure is associated with a decrease in HA; fragments of degraded collagen having being linked to a reduction in *HAS2* synthesis, due to their ability to inhibit the ROCK signalling pathway (Röck *et al.*, 2011). Consequently, it is likely that the qPCR results differ from the TXP analysis due to the differences in exposure time between the HDFn and the skin samples. The HDFn were exposed to one dose of irradiation, which clearly triggered a significant upregulation of HA synthesis, whilst not inducing enough collagen degradation to provide inhibition. However, the skin samples obtained for the TXP analysis, had come from photoexposed sites that had undergone prolonged UV exposure; explaining the decrease in *HAS2* mRNA. As a result, were the experiment to be repeated, and the HDFn exposed to several doses of radiation to mimic chronic exposure, it could be hypothesized that a decrease in *HAS2* would be observed. However, this does not alter the fact that the increase in *HAS2* expression observed in this instance is exceptionally dramatic. Consequently, it does throw into question the validity of the result and it should not be relied upon without the support of further qPCR repeats and additional Western blot analysis; both of which would strengthen the reliability of this observation.

4.2.2 Changes in protein level of ageing biomarkers

Western blot analysis of untreated and irradiated HDFn revealed that X-ray treatment did induce age-related changes in the biomarkers of interest. Elastin was

clearly observed to increase, following irradiation; which coincides with the qPCR results and also the TXP data and current literature on extrinsic ageing which refers to significant elastogenesis following UV exposure (Farage *et al.*, 2008). In addition, the cell cycle inhibitor p21 (CDKN1A) was expressed in HDFn after X-ray treatment, which again matches with the TXP analysis. Moreover, p21 is well established as having a key role in inducing cellular senescence *in vivo*, and it is known to increase following UV exposure (Stoyanova, 2012); making it a key component of extrinsic ageing.

Collagen I was also assessed via Western blot, and it was observed that following irradiation, the amount of alpha 2 chain had decreased slightly. However, the alpha 1 chain produced barely visible bands in both control and irradiated HDFn, and looked as though it might have increased slightly following X-ray treatment. This is interesting, as collagen I molecules are composed of two alpha 1 chains, and one alpha 2 chain; meaning that, if anything, we would have expected to observe slightly more alpha 1 chain than alpha 2 (Rossert *et al.*, 2000). Possible explanations for the weakness of the band, could be that there was not much alpha 1 collagen I extracted from the lysate, or perhaps the use of 5% milk for the antibody diluent was blocking the antigen (Mahmood & Yang, 2012). If that latter was the case, this could perhaps have been rectified by reducing the percentage of milk used, or diluting the antibody in bovine serum albumin (BSA). As a result of this uncertainty, it is likely that the slight increase in the alpha 1 chain following irradiation, is merely due to more antigen being extracted from the lysate, or more antigen being available for antibody binding. As such, it would be unwise to take this result as evidence of a collagen I alpha 1 chain increase following X-ray treatment.

The final biomarker assessed was lamin A/C, which the TXP data showed to increase with age following UV exposure in human skin samples. This correlates with some of the literature on lamin A; studies showing that MMPs may have a role in protecting lamin A from degradation (Limb *et al.*, 2005), and also findings linking lamin A to the DDR due to its role as a binding site for inactive 53-BP1 (Gibbs-Seymour *et al.*, 2015). As UV exposure both increases MMP levels, and DNA damage, it is logical that lamin A would undergo less degradation, and perhaps be overexpressed to enable increased recruitment of 53-BP1. Nonetheless, Western blot analysis revealed that irradiating HDFn led to a decrease in lamin C, and a complete loss of lamin A. Once again, these findings seemed to match more closely with photoprotected ageing; lamin A/C having been found to decrease in the TXP

analysis. At this stage, it is again necessary to draw attention to the fact that X-ray radiation does not necessarily produce the same effects as UV radiation, and therefore the decrease in lamin A/C could be attributed to this distinction. In addition, as mentioned earlier, TXP analysis only provides information on gene expression levels, which does not always match with how much protein is present within a cell (Koussounadis *et al.*, 2015).

However, despite this, the complete loss of lamin A was still unexpected, and its occurrence in all of the repeats discounted the possibility of it being an anomalous result. The role that lamin A has in the normal ageing process is still poorly understood. Whilst mutations in the *LMNA* gene have been associated with premature ageing diseases such as HGPS (Ragnauth *et al.*, 2010), there is very little literature on changes in lamin A/C expression with regard to intrinsic or extrinsic ageing. Some studies have found evidence that progerin is produced in healthy individuals, and that expression increase with age (McClintock, 2007). If true, this could explain a decrease in lamin A protein, as increased use of the cryptic splice site with age would tip the balance of the lamin A:progerin ratio. However, this does not correlate with the findings of this study, as progerin expression was not found to increase following irradiation in HDFn. However, other studies have begun to link accumulation of prelamin A with the ageing process (Ragnauth *et al.*, 2010); observing a correlation between ageing and an overexpression and accumulation of prelamin A. Moreover, build-up of prelamin A has also been associated with an increase in ROS, and accelerated onset of cellular senescence (Sieprath *et al.*, 2015). This could potentially explain the discrepancies between the TXP data and the Western blot result for irradiated HDFn. If prelamin A is overexpressed as cells age, then the gene expression of *LMNA* would increase; as shown in the TXP analysis on photoexposed skin. However, this would not result in an increase in the levels of mature lamin A protein, and only the immature prelamin A would accumulate. Nonetheless, as exciting as this potential theory is, it is in no way conclusive; primarily because the exact specificity of the lamin A/C antibody used in this study is unknown, and it is likely that both prelamin A and mature lamin A were detected in the Western blot. Consequently, it is not currently possible from the literature available, to conclude why lamin A levels were entirely depleted following irradiation. Further analysis could perhaps shed more light on the findings; for example, qPCR would help to ascertain whether loss of lamin A occurred due to gene expression changes, or

post-translational modifications; and use of a prelamin A-specific antibody would enable potential accumulation to be detected.

4.3 Changes in ageing biomarkers in young and old HDF differed from photoexposed TXP results

In order to study a more “*in vivo*-like” experimental group, young and old HDFs were obtained from the Coriell Institute Biorepository. Three young and three old cell lines were used for the analyses, and as all of the old cells were taken from a photoexposed biopsy site, it was hypothesised that changes to ageing biomarkers would follow an extrinsic ageing pattern.

4.3.1 Gene expression changes of ageing biomarkers

As mentioned previously, it is well established that collagens within the skin degrade with age as a result of increased MMP and decreased TIMP production (Fisher *et al.*, 2014). In addition, collagen synthesis decreases as a result of reduced mechanical stimulus from the ECM (Varani *et al.*, 2006). This was observed in the TXP analysis; where both photoprotected and photoexposed skin saw a decrease in the expression of collagens I and IV with age. qPCR analysis of the young and old HDF revealed that both collagen I and collagen IV expression were downregulated in the old cells compared to the young. Whilst collagen I had very clearly diminished, collagen IV had only decreased slightly, and the error bars were very large. However, this did not cause too much concern, because, as has been previously mentioned, collagen IV’s role is in the epidermal basement membrane. As the HDFs were grown in a 2D environment, a basement membrane was not a required structure, and so it is unlikely that the cells would express collagen IV in an *in-vivo*-like manner.

As the young and old HDF were expected to follow the same pattern as photoexposed skin, it was predicted that both elastin and fibrillin 1 expression would increase with age; as shown in the TXP data. Moreover, in the literature, increased expression of elastic fibres is associated with exposure to UV radiation (Langton *et al.*, 2010). However, in the young and old HDF, both elastin and fibrillin 1 expression were observed to decrease with age; following the pattern associated with intrinsic ageing. The potential explanation for these results is that the cells had

been in culture for so long that their biopsy site was no longer relevant. The effects of UV radiation on the skin are very rapid, and dependent on length of exposure time (Seite *et al.*, 2006). The HDF used in this study, were isolated from photoexposed biopsy sites, but then stored and cultured away from UV radiation for a number of years. During this time, without constant exposure to UV, any changes in gene expression or protein levels could only be attributed to processes within the cell; and therefore it is not overly surprising that elastin and fibrillin 1 gene expression changes were observed to follow a pattern associated with photoprotected skin.

Finally, gene expression for HAS2 and TIMP-1 were found to decrease with age, which coincided with the TXP results. However, MMP-1 was shown to decrease dramatically in the old HDF; contradicting both the TXP data, and the majority of literature on ageing and MMP production (Kohl *et al.*, 2011). The likely explanation for this, again draws on the fact that the cells had been in culture for a long time, and the 2D culture environment does not promote gene expression as it would be found *in vivo*. During culture, the old HDF grew very poorly and had to undergo several passages in order to gain enough cells for the required experiments. As a result, they were exposed to an unnatural external environment for a prolonged period of time; much longer than the young HDFs which grew quite rapidly. In human skin, the value given for the Young's Modulus varies depending on technique, but tends to range between low kPa to low MPa (Zahouani *et al.*, 2008). However, plastic tissue cultureware has a Young's Modulus of $E = 0.6 - 3.3$ GPa, depending on the material composition (Cambridge Engineering Department, 2003); up to a staggering 1 million times stiffer than the *in vivo* environment. The rigidity of the ECM can influence gene expression, and culturing cells in a 2D environment has been linked to gene expression perturbation (Birgersdotter *et al.*, 2005). As such, as the old HDF were cultured on a stiff plastic surface for a prolonged period; it is not overly unforeseen that the gene expression patterns do not match with those observed in found in the tissue environment.

4.3.2 Changes in protein level of ageing biomarkers

Western blot analysis was also carried out on young and old HDF, to assess the protein levels of ageing biomarkers. One of the issues that immediately stands out when assessing the results, is the variability between each of the cell lines. The vast heterogeneity of human cells makes them difficult to work with, in that a very large

sample group is required to cancel out the effects of their natural diversity (Rouhani *et al.*, 2014). It is clear that in this study the sample group was much too small to be able to observe clear changes between young and old HDFs. However, the time constraints of the project meant that the pool of useable cells was limited to what was already available, and had been previously worked with. Heterogeneity is affected by both the genetic history of the individual, and also the environmental factors that a person may have been exposed to (Griffiths *et al.*, 2000). In this study, the role of UV radiation is extremely important in influencing the changes in ageing biomarkers between young and old cells. In the analysis, it is assumed that all of the cells were exposed to the same level of UV radiation, but in reality the level of sun exposure would have varied between individuals.

If we put aside the variation within the young and old cell lines, it is possible to identify a few patterns from the Western blot analysis. Firstly, it would appear that levels of elastin decreased slightly in the old cells, which correlates with the qPCR analysis. Moreover, there also seems to be a decrease in the amount of both alpha 1 and alpha 2 chains of collagen I. However, the cell cycle inhibitor p21, was not found to be expressed in any of the cell lines. Whilst the TXP data revealed that p21 increased in both intrinsic and extrinsic ageing; it is in reality a marker of cellular senescence (Passos *et al.*, 2010), and protein lysates were extracted from cells that were still proliferative at the time of harvest. As a result, it is not overly surprising that p21 was not observed in the cells. The final biomarker assessed, was lamin A/C which, according to the TXP analysis, decreases in intrinsic ageing and increases in extrinsic ageing. However, from the Western blot results there does not appear to be any change in lamin A/C levels with age. Once again, a potential explanation for this is the 2D environment that the cells were exposed to. As previously mentioned, the ECM stiffness of the dermis increases slightly with age (Phillip *et al.*, 2015), which has an impact on gene expression within fibroblasts (Solon *et al.*, 2007). However, the young and old HDFs used for this study were cultured for a prolonged period in plastic flasks; meaning that all cell lines were exposed to the same mechanical stimuli; thus potentially explaining why the expected expression changes were not observed. In addition, the potential role of accumulated prelamin A in ageing (Casasola *et al.*, 2016), referred to previously, could explain why TXP results showed an increase in LMNA expression, whilst the Western blot results revealed no change in lamin A levels. However, the issues with antibody specificity remain, and this cannot be concluded.

4.4 Nuclear abnormalities were observed in irradiated and old HDF, but progerin levels showed no change

In the pursuit of fully understanding the ageing process, scientists have begun to investigate links between disease phenotypes, and ageing. A key example of this, is the accelerated ageing disease HGPS; which is caused by a mutation in the *LMNA* gene, leading to a truncated form of prelamin A known as progerin (Ragnauth *et al.*, 2010). Progerin lacks the cleavage site required for the enzyme ZMPSTE24 to remove the protein's farnesyl group; allowing it to be released from the nuclear envelope and form part of the nuclear scaffold (Ragnauth *et al.*, 2010). The presence of progerin in HGPS cells, results in abnormalities in nuclear morphology (Glynn & Glover, 2005), and it has been observed that fibroblasts from old individuals, exhibit similar irregularities in the nuclear envelope (Scaffidi & Misteli, 2006). Further investigation, revealed that progerin is expressed in normal human dermal fibroblasts, and appears to accumulate with age (McClintock *et al.*, 2007).

4.4.1 Nuclear circularity was a poor indicator of nuclear abnormalities

With the literature providing compelling evidence that progerin could have potential as an ageing biomarker, it seemed appropriate to include it in this study; assessing any changes in expression either through age, or exposure to irradiation. Firstly, nuclei were assessed for nuclear abnormalities that could indicate the presence of progerin with the cells. Two methods were utilised for this analysis; a nuclear circularity measurement, and a count of visible irregularities of the envelope. Nuclear circularity calculates the shape of the nucleus using the equation $4\pi \times \text{area}/\text{perimeter}^2$, where a circle = 1.0. It was predicted that irradiation and age would result in a decrease in nuclear circularity; however, results revealed that circularity actually increased in old HDF. In a study into the effects of lamin A mutations on nuclear plasticity, De Vos *et al.* (2010) observed that high passage HDFs from HGPS sufferers actually had better circularity than normal low passage HDFs. Moreover, Choi *et al.* (2011) also found that nuclear circularity was slightly higher in HGPS cells, compared to normal nuclei. Both studies noted that normal nuclei tended to have a more elongated shape, whilst HGPS nuclei were smaller and rounder. When examining the images taken of young and old HDF in this study, it appeared that older nuclei followed a similar pattern of losing their oval shape in

favour of a rounder morphology. This therefore explains why circularity was found to increase in old cells; contrary to expectations. However, despite this, assessment of visual abnormalities revealed that both irradiated HDFn and old HDFs possessed more abnormal nuclei than the control or young cells. As the nuclear circularity was calculated from 2D images, often irregular folds in the envelope were not detected as they occurred across the upper surface of the nuclei, facing the camera. Consequently, it was concluded that nuclear circularity was not an appropriate method of assessing nuclear abnormalities.

4.4.2 The number of nuclear abnormalities did not correlate with progerin levels

Assessment of visible nuclear abnormalities in HDFn and young and old HDFs revealed that irradiated HDFn and old HDFs possessed a greater number of irregular nuclei. As such, it was hypothesized that higher levels of progerin would be observed in these experimental groups. However, Western blot analysis revealed that, whilst progerin was expressed in all cell lines, there was no correlation between irradiation treatment or age, and amount of protein. The presence of increased abnormalities with irradiation and age, suggest that some mechanism is occurring to distort the nuclear envelope. In a study into vascular ageing, Ragnauth *et al.* (2010) observed that *in vitro*, vascular smooth muscle cells (VSMCs) overexpressed and accumulated prelamin A as they aged. Rather than being cleaved by ZMPSTE24, the prelamin A remained at the nuclear envelope and did not migrate to form part of the lamina scaffold. The phenotype observed in HGPS nuclei, is caused by progerin remaining bound to the nuclear envelope by its farnesyl group (Skoczyńska *et al.*, 2015); and thus a build-up of prelamin A would result in the same deformation of the nucleus. Prelamin A accumulation has been associated with accelerated onset of senescence (Ragnauth *et al.*, 2010), and knockdown of the *ZMPSTE24* gene leads to an increase in ROS levels and thus ultimately cellular senescence (Sieprath *et al.*, 2015). Consequently, it appears that, rather than progerin being the cause of the nuclear abnormalities observed in irradiated and old HDFs, it could be that prelamin A accumulation was taking place; contributing to the ageing process by hastening the onset of cellular senescence. This potential scenario seems even more pertinent, when we compare the TXP data for *LMNA* expression, with the Western blot results for lamin A/C protein levels; referred to in sections 4.2 and 4.3.

However, this does not resolve the issue as to why previous studies have identified an increase in progerin with age, yet this was not detected in the irradiated HDFn and old HDFs. Firstly, X-ray irradiation does not have the same wavelength as UV radiation; with UV ranging from 400 nm to 10 nm, whilst X-rays have a wavelength of less than 10 nm (Kusky, 2010). In a study by Takeuchi and Runger (2013), it was discovered that irradiating HDFs with UVB radiation had no effect on progerin expression; however, treating cells with UVA radiation, induced progerin production. Also observed, was that an initial low dose of UVA was not enough to stimulate progerin expression in young cells, only in old; instead, chronic exposure was required before progerin was upregulated in young fibroblasts. Therefore, these data suggest that progerin is only upregulated as a result of exposure to a very specific wavelength; which may explain why irradiating HDFn did not have an effect on progerin levels in the Western blot analysis. Moreover, young cells may require chronic irradiation in order to trigger progerin expression; as this study used neonatal cells that were given a single dose of X-ray, this could also explain why no change in progerin was observed.

Finally, there are some potential explanations as to why old HDFs did not exhibit increased progerin expression. Firstly, we can refer back to the issues that have been discussed previously; such as the long-term culture of the cells on an artificial surface, and the role of mechanical stimuli in controlling gene expression. In other studies, cells have been isolated straight from tissue samples for the purpose of the experiment; therefore minimising the likelihood of changes in cell behaviour as a result of a prolonged period out of the body (Scaffidi & Misteli, 2006 and McClintock *et al.*, 2007). Nevertheless, critical analysis of these reports, does reveal potential weaknesses in the results. For example, McClintock *et al.* (2007) provided a Western blot in which they demonstrated that progerin expression increases with age. However, upon examination, the loading control, β -actin, also appears to increase in the older samples; suggesting that the stronger band for progerin could be due to unequal loading, rather than an actual increase in protein level. Additionally, whilst Scaffidi and Misteli (2006) observed that lamin A/C began to accumulate at the nuclear envelope with age; a feature that could be attributed to progerin's dominant negative effect on lamin A; they did not actually find any evidence of progerin expression increasing with age. Moreover, in a later study, Cao *et al.* (2011) assessed the cause-and-effect relationship of progerin expression in normal ageing, and observed no correlation between age of donor and progerin levels. Consequently, it would appear that the role progerin plays in the normal

ageing process is still very ambiguous, and further study is required before conclusions can be made.

4.5 HDFn cultured on Alvetex[®] scaffolds exhibited some differences in ageing biomarkers compared to 2D cultures

As has been discussed during the analysis of the ageing biomarker data for 2D cultures; growing cells on plastic cultureware is known to differentially activate signalling pathways, and put cells under a great deal of stress (Edmondson, 2014). Consequently, in an effort to provide a more *in vivo*-like environment, HDFn were grown on Alvetex[®] scaffolds to create a dermal equivalent. After 28 days of culture, half of the scaffolds were irradiated with a dose 20 Gy, and the cells were cultured for a further 10 days before being harvested to form lysates. Western blot analysis was then carried out, to assess levels of ageing biomarkers. For both p21, and progerin, the results looked very similar to those observed in the 2D irradiated cells. Firstly, p21 was not expressed in untreated HDFn, but was present in irradiated cells; fitting with the senescent-phenotype known to be produced. Moreover, progerin was again observed to be expressed in both control and irradiated cells, but there appeared to be no correlation between irradiation and level of protein. It has already been mentioned that increased use of the cryptic splice site has been found to be triggered by a specific UV wavelength (Takeuchi & R nger, 2013), so it is likely that no increase in progerin was observed, as X-rays have too short a wavelength to incur a change.

4.5.1 Irradiated 3D cultured HDFn still expressed lamin A

Lamin A/C was also analysed via Western blot for 3D cultures. In the 2D cultures, irradiation induced a decrease in lamin C and a complete loss of lamin A, which could not be explained by any of the current literature. The TXP analysis revealed that expression of lamin A/C increases in photoexposed skin, and decreases in photoprotected skin. In irradiated HDFn cultured on Alvetex[®], lamin C did not appear to change, whilst lamin A decreased slightly. The removal of the cells from a stiff plastic surface, into a porous scaffold, means that it is unlikely to be the effect of the external stimuli that are causing this decrease in expression. A potential explanation might be that the TXP data is not actually representative of the protein level following UV exposure. As mentioned previously, mRNA levels do not always match with protein levels, due to the potential for post-translational modifications and degradation (Maier *et al.*, 2009). It has been documented that lamin A acts as a

binding site for the DNA damage repair protein 53BP1 (Gibbs-Seymour *et al.*, 2015). In the absence of lamin A, 53BP1 is destabilised (Redwood *et al.*, Aug. 2011); a process that has been linked to the role lamin A has in suppressing the cysteine protease cathepsin L (CTSL) (Redwood *et al.*, Nov. 2011). In the absence of lamin A, CTSL is upregulated; resulting in increased degradation of 53BP1 (Redwood *et al.*, Nov. 2011). Consequently, it could be hypothesised that in response to the DNA damage caused by UV exposure, lamin A expression is upregulated in order to decrease CTSL levels; thus maximising the available 53BP1.

However, at a protein level, lamin A has also been associated with ROS. Pekovic *et al.* (2011) observed that lamin A contains unique cysteine residues that form disulphide bonds following exposure to mild oxidative stress; resulting in temporary growth arrest without changes in nuclear morphology, or increased expression of (SA)- β -gal. However, following exposure to severe levels of ROS, disulphide bonds did not form, and cells entered cellular senescence; accompanied by a significant increase in the number of abnormal nuclei. Consequently, this suggests that there is some mechanism that takes place following excessive oxidative stress, that prevents lamin A from carrying out its seemingly protective role, and pushes cells into full senescence. As the results of this study showed lamin A decreasing following irradiation, it could perhaps have something to do with a diminished level of lamin A protein. However, lamin A's true part in the ageing process is still very poorly understood. Nevertheless, the fact that lamin A was entirely lost in irradiated HDFn grown in 2D, but only decreased in 3D cells, suggests that 3D culture potentially provides an environment that enabled the cells to better resist the impact of external stresses; perhaps because they were in a healthier state when first exposed to irradiation.

4.5.2 3D cultured HDFn produced a single band for collagen I in Western blot analysis

Collagen I is formed of a triple helix comprised from two alpha 1 chains, and one alpha 2 chain (Brosky & Persikov, 2005). These alpha chains are both detected by the antibody used, and are observed as two separate bands in the 2D Western blot analysis for both HDFn and young and old HDF. However, in the 3D Western blot result, only one band was observed in both control and irradiated HDFn. At first, it was considered that this could be the alpha 2 chain, as the alpha 1 chain was very

faint, or even absent in some of the 2D data. However, the band was not the correct weight for this; being approximately 250 kDa, whilst alpha 1 is 139 kDa, and alpha 2 is 129 kDa. As this antibody has been shown to work previously, the most logical explanation is that the band found in the results, represents a protein dimer.

The chains of the triple helix are initially joined by disulphide bonds, which are usually broken down in Western blots by the addition of reducing agents such as mercaptoethanol (2.6.3). However, in order control the pH of the samples during the stacking and resolving stages, the buffer Laemmli is added. The pH values promoted by this buffer can lead to the creation of new disulphide bonds; and therefore, it is important that the balance between buffer and reducing agent is such that bonds cannot form (Boster, undated). It is possible that the cause of the band observed in the results, was due to not enough mercaptoethanol being added to the samples; resulting in some disulphide bond formation. However, one issue with this theory, is the absence of any other bands on the gel; if a dimer had been formed, the remaining chain from the original trimer should still appear. Moreover, the band was observed to be stronger following irradiation; contradicting current literature, the TXP data, and all other results obtained in this study regarding collagen I. Consequently, the origins of the band remain inconclusive, and repetition of the experiment, followed by further analysis, would be required in order to make any conclusions.

4.6 Analysis of human skin samples revealed the same changes in biomarkers as observed *in vitro*

The final aspect of this study, was to compare the results achieved *in vitro*, with human skin samples; in order to see whether ageing biomarkers could truly be used to help in the development of an aged skin model. Whilst the TXP data was obtained from human skin; due to the risk of mRNA levels failing to represent the amount of protein (Koussounadis *et al.*, 2015), it was important to assess changes in ageing biomarkers through another mechanism. Human skin samples from young and old donors (provided by P&G), were immunostained for the biomarkers collagen I, collagen IV, elastin, and lamin A. Strikingly, the changes observed in old skin, were identical to the results obtained for irradiated HDFn, with the exception of the qPCR result for collagen IV, which was discussed earlier. Both collagens I and IV were seen to decrease in old skin samples; whilst elastin levels increased and fibre aggregation was observed. In addition, lamin A/C levels also appeared to

decrease, which was again consistent with the results seen for HDFn *in vitro*. Consequently, it seems pertinent to suggest that irradiated HDFn are a good model of skin ageing; and as such could be used to make a tissue model. Moreover, the young and old HDFs also showed some similar changes to human skin; elastin increasing slightly, whilst collagen I decreased. As such, with newer cell lines, the use of young and old also fibroblasts could also make a reliable skin model; though the culture time would be significantly increased in comparison to an irradiated model.

5. Conclusions and Future Directions

Human dermal fibroblasts, taken from young and old donors and grown *in vitro*, exhibit tissue-like changes in the expression of ageing biomarkers. Moreover, irradiating HDFn with a dose of 20 Gy, induces a senescent state that also reflects *in vivo* ageing. Occasional discrepancies in biomarker expression, could be attributed to the use of plastic cultureware; future work should be continued in 3D, in order to promote development of an aged skin model. Where the cells did not match the TXP data obtained from human skin, they did match the expression observed in immunostained skin samples. This suggests a potential post-translational mechanism between mRNA and protein; necessitating that future investigations should consist of both qPCR and Western blot analysis for every biomarker assessed. Whilst this study was focused on investigating the dermal compartment of skin, in order to truly create a physiologically relevant model, a similar study into ageing biomarkers should be completed on epidermal equivalents. The eventual development of a full thickness aged model of skin, would be the final step in enabling *in vitro* ageing analysis.

All cells were observed to express a low level of progerin; revealing that the cryptic splice site is occasionally utilised by healthy cells. However, there was no observed correlation between irradiation or cell donor age, and level of progerin; thus meaning that it was not possible to conclude that progerin is an ageing biomarker. Nonetheless, this could be further investigated by using a splice reporter to monitor how often the cryptic splice site is employed; thus ruling out any potential post-translational interference. In addition, some literature suggests that it is potentially prelamin A accumulation that causes the dysmorphic nuclear shape observed in old cells. This could be assessed by the use of a specific prelamin A antibody; which would provide information on its potential as an ageing biomarker.

References

- Achterberg, V.F *et al.*, (2014). "The Nano-Scale Mechanical Properties of the Extracellular Matrix Regulate Dermal Fibroblast Function." *Journal of Investigative Dermatology*, **134**(7), p1862-1872.
- Agami, R. and Bernards, R., (2000). "Distinct Initiation and Maintenance Mechanisms Cooperate to Induce G1 Cell Cycle Arrest in Response to DNA Damage." *Cell*, **102**(1), p55-66.
- Alam, S., *et al.*, (2014). "Nuclear Forces and Cell Mechanosensing." *Progress in molecular biology and translational science*, **126**, p205–215.
- Angenete E. *et al.*, (2009). "Preoperative radiotherapy and extracellular matrix remodeling in rectal mucosa and tumour matrix metalloproteinases and plasminogen components." *Acta Oncologica*, **48**, p1144-1151.
- Baker, G.T. and Sprott, R.L., (1988). "Biomarkers of ageing." *Experimental Gerontology*, **23**, p223-239.
- Baron, J.M. *et al.*, (2005). "Retinoic Acid and its 4-Oxo Metabolites are Functionally Active in Human Skin Cells In Vitro." *Journal of Investigative Dermatology*, **125**, p143-153.
- Battie, C. *et al.*, (2014). "New insights in photoaging, UVA induced damage and skin types." *Experimental Dermatology*, **23**(1), p7-12.
- Baumann, L., (2007). "Skin ageing and its treatment." *The Journal of Pathology*, **211**(2), p241-251.
- Birgersdotter, A. *et al.*, (2005). "Gene expression perturbation in vitro—A growing case for three-dimensional (3D) culture systems." *Seminars in Cancer Biology*, **15**(5), p405-412.
- Boster, (undated). "Western Blot Principle." Available at: <https://www.bosterbio.com/protocol-and-troubleshooting/western-blot-principle> [Accessed 11 Oct. 2016].
- Brodsky, B. and Persikov, A.V., (2005). "Molecular Structure of the Collagen Triple Helix." *Advances in Protein Chemistry*, **70**, p301-339.
- Brohem, C.A. *et al.*, 2011. "Artificial Skin in Perspective: Concepts and Applications". *Pigment Cell & Melanoma Research*, **24**(1), p35-50.
- Brun, C. *et al.*, (2016). "Phenotypic and functional changes in dermal primary fibroblasts isolated from intrinsically aged human skin." *Experimental Dermatology*, **25**(2), p113-119
- Calleja-Agius, J. *et al.*, (2013). "Skin connective tissue and ageing." *Best Practice & Research Clinical Obstetrics & Gynaecology*, **27**(5), p727-740.

Cambridge Engineering Department, (2003). "Material Data Book." Available at: <http://www-mdp.eng.cam.ac.uk/web/library/enginfo/cueddatabooks/materials.pdf> [Accessed 09 Oct. 2016].

Cao, K. *et al.*, (2011). "Progerin and telomere dysfunction collaborate to trigger cellular senescence in normal human fibroblasts." *The Journal of Clinical Investigation*, **121**(7), p2833-2844.

Casasola, A. *et al.*, (2016). "Prelamin A processing, accumulation and distribution in normal cells and laminopathy disorders." *Nucleus*, **7**(1), p84-102.

Choi, S. *et al.*, (2011). "Computational image analysis of nuclear morphology associated with various nuclear-specific aging disorders." *Nucleus*, **2**(6), p570-579.

Dalle Pezze, P., *et al.* (2014). "Dynamic Modelling of Pathways to Cellular Senescence Reveals Strategies for Targeted Interventions." *PLoS Computational Biology*, **10**(8), e1003728.

Debacq-Chainiaux, F. *et al.*, 2009. "Protocols to detect senescence-associated beta-galactosidase (SA-[beta]gal) activity, a biomarker of senescent cells in culture and in vivo." *Nature Protocols*, **4**(12), p1798-1806.

De Vos, W.H. *et al.*, (2010). "Increased plasticity of the nuclear envelope and hypermobility of telomeres due to the loss of A-type lamins." *Biochimica et Biophysica Acta – General Subjects*, **1800**(4), p448-458.

Dos Santos, M. *et al.*, (2015). "In vitro 3-D model based on extending time of culture for studying chronological epidermis ageing." *Matrix Biology*, **47**, p85-97.

Edmondson R. *et al.*, (2014). "Three-Dimensional Cell Culture Systems and Their Applications in Drug Discovery and Cell-Based Biosensors." *Assay and Drug Development Technologies*, **12**(4), p.207-218.

Farage, M.A. *et al.*, (2008). "Intrinsic and extrinsic factors in skin ageing: a review." *International Journal of Cosmetic Science*, **30**(2), p87-95.

Faratian, D. *et al.*, (2009). "Membranous and cytoplasmic staining of Ki67 is associated with HER2 and ER status in invasive breast carcinoma." *Blackwell Publishing Ltd*, **54**(2), p254-257.

Finkelstein, J. N. *et al.*, (1994). "Early alterations in extracellular matrix and transforming growth factor gene expression in mouse lung indicative of late radiation fibrosis." *International Journal of Radiation Oncology * Biology * Physics*, **28**, p621–631.

Fisher, G.J. *et al.*, (2009). "Collagen Fragmentation Promotes Oxidative Stress and Elevates Matrix Metalloproteinase-1 in Fibroblasts in Aged Human Skin." *The American Journal of Pathology*, **174**(1), p101-114.

Fisher, G.J. *et al.*, (2014). "Ageing: collagenase-mediated collagen fragmentation as a rejuvenation target." *British Journal of Dermatology*, **171**(2), p1365-2133.

- Gibbs-Seymour, I. *et al.*, (2015). "Lamin A/C-dependent interaction with 53BP1 promotes cellular responses to DNA damage." *Aging Cell*, **14**, p162-169.
- Gerecht, S. *et al.*, (2007). "Hyaluronic acid hydrogel for controlled self-renewal and differentiation of human embryonic stem cells." *PNAS*, **104**(27), p11298-11303.
- Glynn, M.W. and Glover, T.W., (2005). "Incomplete processing of mutant lamin A in Hutchinson–Gilford progeria leads to nuclear abnormalities, which are reversed by farnesyltransferase inhibition." *Human Molecular Genetics*, **14**(2), p2969-2969.
- Gonzalo-Calvo, D. *et al.*, (2010). "Differential inflammatory responses in aging and disease: TNF- α and IL-6 as possible biomarkers." *Free Radical Biology and Medicine*, **49**(5), p733-737
- Griffiths, A.J.F., *et al.*, (2000). "An Introduction to Genetic Analysis." 7th edition. New York: W. H. Freeman; Genes, the environment, and the organism.
- Halliday, G.M., (2005). "Inflammation, gene mutation and photoimmunosuppression in response to UVR-induced oxidative damage contributes to photocarcinogenesis." *Mutation Research/Fundamental and Molecular Mechanisms of Mutagenesis*, **571**(1-2), p107-120.
- Hee Lee, W. *et al.*, (2012). "Irradiation Alters MMP-2/TIMP-2 System and Collagen Type IV Degradation in Brain." *International Journal of Radiation Oncology*Biophysics*, **82**(5), p1559-1566.
- Heise, R., *et al.*, (2006). "Skin Retinoid Concentrations Are Modulated by CYP26A1 Expression Restricted to Basal Keratinocytes in Normal Human Skin and Differentiated 3D Skin Models." *Journal of Investigative Dermatology*, **126**(11), p2473-2480.
- Jean, J. *et al.*, (2011). "Bioengineered Skin: The Self-Assembly Approach." *Journal of Tissue Science and Engineering*, **5**(001).
- Jenkins, G., (2002). "Molecular mechanisms of skin ageing." *Mechanisms of Ageing and Development*, **123**(7), p801-810.
- Johnson, T.E., (2006). "Recent results: Biomarkers of aging." *Experimental Gerontology*, **41**(12), p1243-1246.
- Jung, Y-S. *et al.*, (2013). "Loss of *VHL* promotes progerin expression, leading to impaired p14/ARF function and suppression of p53 activity." *Cell Cycle*, **12**(14), p2277-2290.
- Kim D. *et al.*, (2015). "Epidermal growth factor improves the migration and contractility of aged fibroblasts cultured on 3D collagen matrices." *International Journal of Molecular Medicine*, **35**(4), p1017-1025.
- Knight, E., *et al.*, (2011). "Alvetex[®]: Polystyrene Scaffold Technology for Routine Three Dimensional Cell Culture." *3D Cell Culture, Methods in Molecular Biology*, **695**, p323-340.

- Knight, E. and Przyborski, S., (2014). "Advances in 3D cell culture technologies enabling tissue-like structures to be created *in vitro*." *Journal of Anatomy*, **227**(6), p746-756.
- Kohl, E. *et al.*, (2011). "Skin ageing." *Journal of the European Academy of Dermatology and Venereology*, **25**(8), p873-884.
- Koussounadis, A. *et al.*, (2015). "Relationship between differentially expressed mRNA and mRNA-protein correlations in a xenograft model system." *Scientific Reports*, **5**.
- Kusky, T., (2010). "Encyclopedia of Earth and Space Science." New York: Facts on File, Inc; p245-246.
- Langton, A. *et al.*, (2010). "Review Article: A new wrinkle on old skin: the role of elastic fibres in skin ageing." *International Journal of Cosmetic Science*, **32**(5), p330-339.
- Leontieva, O.V., *et al.*, (2010). "Weak p53 permits senescence during cell cycle arrest." *Taylor & Francis*, **9**(21), p4323-4327.
- Limb, G.A. *et al.*, (2005). "Matrix Metalloproteinase-1 Associates with Intracellular Organelles and Confers Resistance to Lamin A/C Degradation during Apoptosis." *The American Journal of Pathology*, **166**(5), p1555-1563.
- Mahmood, T and Yang, P-C., (2012). "Western Blot: Technique, Theory and Troubleshooting." *North American Journal of Medical Sciences*, **4**(9), p429-434.
- Maier, T. *et al.*, (2009). "Correlation of mRNA and protein in complex biological samples." *FEBS Letters*, **583**(24), p3966-3973.
- Maltman, D.J. and Przyborski, S.A., (2010). "Developments in three-dimensional cell culture technology aimed at improving the accuracy of *in vitro* analyses." *Biochemical Society Transactions*, **38**(4), p1072-1075.
- Mancini, M. *et al.*, (2014). "MicroRNAs in human skin ageing." *Ageing Research Reviews*, **17**, p9-15.
- Masaki, H., (2010). "Role of antioxidants in the skin: Anti-aging effects." *Journal of Dermatological Science*, **58**(2), p 85-90.
- McClintock, D, *et al.*, (2007). "The Mutant Form of Lamin A that Causes Hutchinson-Gilford Progeria Is a Biomarker of Cellular Aging in Human Skin." *PLoS ONE*, **2**(12), e1269.
- Meredith, M.A. *et al.*, (2008). "Phenotype and Course of Hutchinson-Gilford Progeria Syndrome." *The New England Journal of Medicine*, **358**, p592-604.
- Michel, M. *et al.*, (1999). "Characterization of a new tissue-engineered human skin equivalent with hair." *In Vitro Cellular & Developmental Biology – Animal*, **35**(6), p318-326.
- Miyagi, Y. *et al.*, (2011). "Biodegradable collagen patch with covalently immobilized VEGF for myocardial repair." *Biomaterials*, **32**(5), p1280-1290.

- Naylor, E.C. *et al.*, (2011). "Molecular aspects of skin ageing." *Maturitas*, **69**(3), p249-256.
- Oh, J-H. *et al.*, (2011). "Intrinsic aging- and photoaging-dependent level changes of glycosaminoglycans and their correlation with water content in human skin." *Journal of Dermatological Science*, **62**(3), p192-201.
- Papakonstantinou, E. *et al.*, (2012). "Hyaluronic acid: A key molecule in skin ageing." *Dermato-Endocrinology*, **4**(3), p253-258.
- Park, M.Y. *et al.*, (2010). "Photorejuvenation induced by 5-aminolevulinic acid photodynamic therapy in patients with actinic keratosis: A histologic analysis." *Journal of the American Academy of Dermatology*, **62**(1), p85-95.
- Passos, J.F. *et al.*, (2010). "Feedback between p21 and reactive oxygen production is necessary for cell senescence." *Molecular Systems Biology*, **6**(1).
- Pekovic, V. *et al.*, (2011). "Conserved cysteine residues in the mammalian lamin A tail are essential for cellular responses to ROS generation." *Anatomical Society*, **10**(6), p1067-1069.
- Phillip, J.M., *et al.* (2015). "The Mechanobiology of Aging." *Annual review of biomedical engineering*, **17**, p113-141.
- Poljšak, B. and Dahmane, R. (2012). "Free Radicals and Extrinsic Skin Aging." *Dermatology Research and Practice*, p1-4.
- Poljšak, B. *et al.*, (2012). "Intrinsic ageing: The role of oxidative stress." *Acta Dermatovenerol APA*, **21**, p1-4.
- Proksch, E. *et al.*, (2008). "The skin: an indispensable barrier." *Experimental Dermatology*, **17**, p1063–1072.
- Ragnauth, C.D. *et al.*, (2010). "Prelamin A Acts to Accelerate Smooth Muscle Cell Senescence and Is a Novel Biomarker of Human Vascular Aging." *Circulation*, **121**(20).
- Redwood, A.B. *et al.*, (2011). "A dual role for A-type lamins in DNA double-strand break repair." *Cell Cycle*, **10**(15), p2549-2560.
- Redwood, A.B. *et al.*, (2011). "Regulating the levels of key factors in cell cycle and DNA repair: New pathways revealed by lamins." *Cell Cycle*, **10**(21), p3652-3657.
- Ressler, S. *et al.*, (2006). "p16^{INK4A} is a robust *in vivo* biomarker of cellular aging in human skin." *Aging Cell*, **5**(5), p379-389.
- Reuter, S. *et al.*, (2010). "Oxidative stress, inflammation, and cancer: How are they linked?." *Free Radical Biology and Medicine*, **49**(11), p1603-1616.
- Röck, K. *et al.*, (2011). "Collagen Fragments Inhibit Hyaluronan Synthesis in Skin Fibroblasts in Response to Ultraviolet B (UVB)." *The Journal of Biological Chemistry*, **286**(20), p18268–18276.

- Rodier, F. and Campisi, J., (2011). "Four faces of cellular senescence." *The Journal of Cell Biology*, **192**(4), p547-556.
- Rouhani F., *et al.* (2014). "Genetic Background Drives Transcriptional Variation in Human Induced Pluripotent Stem Cells." *PLoS Genetics*, **10**(6).
- Rossert, J. *et al.*, (2000). "Regulation of type I collagen genes expression." *Nephrology Dialysis Transplantation*, **15**(6), p66-68.
- Scaffidi P, Misteli T (2006). "Lamin A-Dependent Nuclear Defects in Human Aging." *Science*, **312**(5776), p1059-1063.
- Seite, S. *et al.*, (2006). "Elastin changes during chronological and photo-ageing: the important role of lysozyme." *Journal of the European Academy of Dermatology and Venereology*, **20**(8), p980-987.
- Shay, J.W. and Wright, W.E., (2000). "Hayflick, his limit, and cellular ageing." *Nature Reviews Molecular Cell Biology*, **1**, p72-76.
- Sieprath, T. *et al.*, (2015). "Sustained accumulation of prelamin A and depletion of lamin A/C both cause oxidative stress and mitochondrial dysfunction but induce different cell fates." *Nucleus*, **6**(3), p236-246.
- Siiskonen, H. *et al.*, (2015). "Hyaluronan Synthase 1: A Mysterious Enzyme with Unexpected Functions." *Frontiers in Immunology*, **6**(43).
- Skoczyńska, A. *et al.*, (2015). "New look at the role of progerin in skin ageing." *Menopause Review*, **14**(1), p53-58.
- Solon, J. *et al.*, (2007). "Fibroblast Adaptation and Stiffness Matching to Soft Elastic Substrates." *Biophysical Journal*, **93**(12), p4453-4461.
- Stöckl P. *et al.*, (2006). "Sustained inhibition of oxidative phosphorylation impairs cell proliferation and induces premature senescence in human fibroblasts." *Experimental Gerontology*, **41**(7), p674-682
- Stoyanova T. *et al.*, (2012). "p21 Cooperates with DDB2 Protein in Suppression of Ultraviolet Ray-induced Skin Malignancies." *The Journal of Biological Chemistry*, **287**(5), p3019-3028.
- Suzuki, K. *et al.* (2001). "Radiation-Induced Senescence-like Growth Arrest Requires TP53 Function but not Telomere Shortening." *Radiation Research*, **155**(1), p248-253.
- Takeuchi, H. and Rütger, T.M., (2013). "Longwave UV Light Induces the Aging-Associated Progerin." *Journal of Investigative Dermatology*, **133**(7), p1857-1862.
- Tang Y., *et al.*, (2010). "Promotion of tumor development in prostate cancer by progerin." *Cancer Cell International*, **10**(47).

Tasdemir, N. and Lowe, S.W., (2013). "Senescent cells spread the word: non-cell autonomous propagation of cellular senescence." *The EMBO Journal*, **32**(14), p1975-1976.

Tsourelis-Nikita, E. *et al.*, (2006). "Photoageing: the darker side of the sun." *Photochemical and Photobiological Sciences*, **5**, p160-164.

Varani, J. *et al.*, (2006). "Decreased Collagen Production in Chronologically Aged Skin: Roles of Age-Dependent Alteration in Fibroblast Function and Defective Mechanical Stimulation." *The American Journal of Pathology*, **168**(6), p1861-1868.

Watson, R.E.B. *et al.*, (2001). "A Short-Term Screening Protocol, Using Fibrillin-1 as a Reporter Molecule, for Photoaging Repair Agents." *Journal of Investigative Dermatology*, **116**, p672-678.

Wu, M. *et al.*, (2011). "Effect of aging on cellular mechanotransduction." *Ageing research reviews*, **10**(1), p1-15.

Wu, Y. *et al.*, (2000). "The proteasome controls the expression of a proliferation-associated nuclear antigen Ki-67." *Journal of Cellular Biochemistry*, **76**(4), p596-604.

Yavas, G. *et al.*, (2014). "Ionizing Radiation Induces Cytokines, MMP-1, TIMP-1 and Suppresses Type I Collagen mRNA Expressions in Human Gingival Fibroblasts." *International Journal of Hematology and Oncology*, **24**(3), p149-156.

Zahouani, H. *et al.*, (2009). "Characterization of the mechanical properties of a dermal equivalent compared with human skin in vivo by indentation and static friction tests." *Skin Research and Technology*, **15**(1), p68-76.

Zglinicki, T. *et al.*, (2005). "Human cell senescence as a DNA damage response." *Functional Genomics of Ageing II*, **126**(1), p111-117.

Znati, C.A. *et al.*, (2003). "Irradiation Reduces Interstitial Fluid Transport and Increases the Collagen Content in Tumors." *Clinical Cancer Research*, **9**, p5508-5513.